

Journal: ACP

Title: Optical properties and molecular compositions of water-soluble and water-insoluble brown carbon (BrC) aerosols in Northwest China

Author(s): Jianjun Li et al.

MS No.: acp-2019-1002

Dear Editor,

After reading the comments from the two referees, we have carefully revised our manuscript. Our response to the comments and related revisions are attached with this letter.

Anything about our paper, please feel free to contact me at dkwzhang@ucdavis.edu.

Best regards,

Sincerely yours

Qi Zhang

Mar. 18, 2020

Anonymous Referee #2

This paper presents measurements of water soluble and insoluble brown carbon (BrC) in different seasons in Guangzhong Basin in China. The possible sources and radiative effects of BrC are also discussed. The paper is well written and within the scope of ACP. I would recommend the publication of this manuscript in ACP if the comments below are well addressed.

Response: We thank the referee's comments, which are very helpful for us to improve our work. Detailed revision and response to the comments are listed below.

Specific comments:

L148: delete "and"

Response: Suggestion taken. Please see Line 150.

L171: Can the author give an estimate of the bias of $MAC_{\lambda, WI-BrC}$ in your measurement. It would be also good to provide measurement uncertainties of other derived parameters.

Response: We thank the referee's suggestion. We added the uncertainties of $Abs_{\lambda, WI-BrC}$ and $MAC_{\lambda, WI-BrC}$ in the revised manuscript. (Please see Line 173-174)

L192: Can the author give some details of why 1.3 was used?

Response: We thank the referee's suggestion. More details were provided in Line 196-205.

L203: how do these numbers compare with the measurement in other polluted regions (e.g. NCP, PRD and YRD) in China?

Response: We thank the referee's comment. We added a comparison of AAE value measured in this study with those in typical cities in NCP, PRD and YRD, please see Line 222-224.

L219: Since there is a tip at 360 and definitely influences 365, maybe it is better to use another wavelength for reporting abs?

Response: We do agree with the referee's comment. So we added a table (Table S1) to compare the Abs and MAC in wavelength of 340-380 nm. We found that the influence of the tip seems insignificant on the average Abs_{365} or MAC_{365} . Thus, in order to be consistent with previous studies, we still use 365 nm for reporting Abs and MAC, and gave a detailed explanation at Line 251-254.

L221: I would not call it "significant higher"

Response: Suggestion taken. We revised to "much higher" in Line 266.

L236: Since your site represents regional background conditions (is it?), how these

numbers compare with other regional background measurements?

Response: We thank the referee's comment. We added a comparison with some data reported in other regional or background sites in China, please see Line 260-262 and Table 2.

L311-315: Why is levoglucosan concentration much higher in daytime than in nighttime in summer? $Abs_{365, WI-BrC}$ shows higher R² with levoglucosan concentration. Does it mean POA from biomass burning is also an important contributor to BrC in daytime in summer? I think based only on the correlations, it is difficult to judge if primary emission or photochemical formation is more important.

Response: We thank the referee's comment. Yes, the concentration of levoglucosan is also higher in daytime than in nighttime in summer due to enhanced emission from BB for domestic cooking. As described in Line 303-305, " $Abs_{365, WI-BrC}$ in both summer and winter correlate well with levoglucosan ($r^2=0.74$ and 0.62 , respectively), demonstrating an important contribution of biomass burning to WI-BrC...". However, we cannot quantitatively judge if primary emission or photochemical formation is more important for WI-BrC in summer. Thus in "Conclusion", we concluded that "These results demonstrated that photochemical formation of BrC and enhanced BB emissions (e.g., from cooking) contributed to the higher daytime MACs in summer" (Line 495-497). Moreover, to avoid the confusion, we also revised the sentence "This difference was mainly attributed to enhanced photochemical formation of WI-BrC species, such as oxygenated polycyclic aromatic hydrocarbons (OPAHs)" in the Abstract to "This difference was partly attributed to enhanced photochemical formation of WI-BrC species, such as oxygenated polycyclic aromatic hydrocarbons (OPAHs)" (Line 42-43).

L398: Correlations with RH, sulfate and NO₂ do not necessarily mean that aqueous oxidation has played a role in the formation of WS-BrC. We can see WI-BrC shows the same trend during the period. During haze event, the stagnant meteorological condition with low wind speed promotes the accumulation of BrC no matter how it is produced.

Response: We thank the referee's comment. Indeed, the correlations of $Abs_{365, WS-BrC}$ with RH, sulfate and NO₂ are not necessarily to prove the aqueous formation of WS-BrC. However, we have more evidence for this. Firstly, the temporal variation of $Abs_{365, WI-BrC}$ and $Abs_{365, WS-BrC}$ is actually different. $Abs_{365, WS-BrC}$ increases continuously during the haze period, whereas $Abs_{365, WI-BrC}$ presents obvious diurnal variation (Figure 1). Secondly, the relationship of RH, sulfate and NO₂ with $Abs_{365, WS-BrC}$ are much stronger than those with $Abs_{365, WI-BrC}$, but levoglucosan and PAHs have stronger correlation with $Abs_{365, WI-BrC}$. These results suggested that $Abs_{365, WI-BrC}$ were more related with primary emissions, but aqueous oxidation was an important source for WS-BrC. In addition, in our previous study in Xi'an (~40 km away from the sampling site in this study), we further analyzed the stable carbon isotope composition and also found a secondary formation of BrC in winter (Wu et al., 2020). Thus, we confirmed that aqueous oxidation has played a role in the

formation of WS-BrC. More detailed description also added in the manuscript, please see Line 423-430.

Figure 2e and f not mentioned in the text.

Response: We thank the referee's reminder. Figure 2e and f were deleted in the revised manuscript.

Reference

Wu, C., Wang, G., Li, J., Li, J., Cao, C., Ge, S., Xie, Y., Chen, J., Li, X., Xue, G., Wang, X., Zhao, Z., and Cao, F.: The characteristics of atmospheric brown carbon in Xi'an, inland China: sources, size distributions and optical properties, *Atmos. Chem. Phys.*, 20, 2017-2030, 10.5194/acp-20-2017-2020, 2020.

Anonymous Referee #3

In this work, the authors examined the absorption properties and molecular compositions of water-soluble and –insoluble PM_{2.5} brown carbon from a rural site in China. Seasonal variation, day time vs night time, as well as water-soluble vs water-insoluble of absorbance and MAC values of particles were discussed. Their results showed the contribution of photochemical formation of brown carbon and biomass burning emissions to higher daytime MACs in summer in the region. They also suggest the important role of aqueous-phase reactions and nitrated aromatic compounds in the formation of secondary brown carbon. Overall, the authors have done a great job in analyzing and discussing their data. The work is also well presented. I recommend acceptance.

Response: We thank the referee's comments.

Specific comments:

1) Line 120 should it be “_8am to 8pm”?

Response: Suggestion taken. Please see Line 121.

2) Section 2.4 please indicate where to subtract the signal from blanks in your calculations.

Response: We thank the referee's comment. We added the information at Line 163-164.

3) Line 170 what is M in Eq. 3?

Response: We thank the referee's comment. We added an explanation about M in Eq. 3, please see 172.

4) Line 222 “Abs₃₆₅ of WS-BrC is significantly higher than WI-BrC in summer, but values are comparable in winter”. However, Figure 2 shows Abs₃₆₅ of WI-BrC is higher than WS-BrC in winter. Please explain.

Response: We thank the referee's comment. The averaged value of Abs₃₆₅ of WI-BrC and WS-BrC in winter were $19.6 \pm 8.3 \text{ Mm}^{-1}$ and $21.9 \pm 13.5 \text{ Mm}^{-1}$, respectively. So we revised the sentence as “On average, Abs_{365,WS-BrC} is significantly higher than Abs_{365,WI-BrC} in summer ($5.00 \pm 1.28 \text{ Mm}^{-1}$ vs. $2.95 \pm 1.94 \text{ Mm}^{-1}$), but the values vary slightly in winter ($19.6 \pm 8.3 \text{ Mm}^{-1}$ vs. $21.9 \pm 13.5 \text{ Mm}^{-1}$)” (Line 240-242).

5) Line 405 an increase of MAC₃₆₅ during New Year's Eve was observed but an increase of Abs₃₆₅ or PM mass or WSOC was NOT observed. Please explain.

Response: We thank the referee's comment. The increase of Abs₃₆₅ or PM mass or WSOC was NOT observed because the metrological condition were favoring for pollutants dispersion (Figure 1). Thus, we provided more detailed explanation at Line 436-440.

1 **Optical properties and molecular compositions of water-soluble and water-**
2 **insoluble brown carbon (BrC) aerosols in Northwest China**

3
4 Jianjun Li^{1,2}, Qi Zhang^{2,*}, Gehui Wang^{1,3,4,*}, Jin Li¹, Can Wu^{1,3}, Lang Liu¹, Jiayuan Wang^{1,2},
5 Wenqing Jiang², Lijuan Li^{1,2}, Kin Fai Ho^{1,5}, Junji Cao¹

6
7 ¹ Key Lab of Aerosol Chemistry & Physics, SKLLQG, Institute of Earth Environment, Chinese
8 Academy of Sciences, Xi'an 710061, China

9 ² Department of Environmental Toxicology, University of California, Davis, CA 95616, USA

10 ³ Key Laboratory of Geographic Information Science of the Ministry of Education, School of
11 Geographic Sciences, East China Normal University, Shanghai 200241, China

12 ⁴ Institute of Eco-Chongming, 3663 N. Zhongshan Rd., Shanghai 200062, China

13 ⁵ The Jockey Club School of Public Health and Primary Care, The Chinese University of Hong
14 Kong, Hong Kong, China

15
16
17 *Corresponding authors:

18 Prof. Qi Zhang

19 Department of Environmental Toxicology, University of California, Davis

20 One Shields Avenue, Davis, CA 95616

21 Phone: 1-530-752-5779

22 Fax: 1-530-752-3394

23 Email: dkwzhang@ucdavis.edu;

24
25 Prof. Gehui Wang

26 School of Geographic Sciences, East China Normal University, Shanghai, China

27 500 Dongchuan Rd., Shanghai 200241, China

28 Phone: 86-21-5434-1193

29 E-mail: ghwang@geo.ecnu.edu.cn.

30

31 Abstract

32 Brown carbon (BrC) contributes significantly to aerosol light absorption, thus can affect the earth's
33 radiation balance and atmospheric photochemical processes. In this study, we examined the light
34 absorption properties and molecular compositions of water-soluble (WS-BrC) and water-insoluble
35 (WI-BrC) BrC in PM_{2.5} collected from a rural site in the Guanzhong Basin – a highly polluted
36 region in Northwest China. Both WS-BrC and WI-BrC showed elevated light absorption
37 coefficients (Abs) in winter (4-7 times of those in summer) mainly attributed to enhanced
38 emissions from residential biomass burning (BB) for house heating. While the average mass
39 absorption coefficients at 365 nm (MAC₃₆₅) of WS-BrC were similar between daytime and
40 nighttime in summer (0.99 ± 0.17 and 1.01 ± 0.18 m² g⁻¹, respectively), the average MAC₃₆₅ of WI-
41 BrC was more than a factor of 2 higher during daytime (2.45 ± 1.14 m² g⁻¹) than at night (1.18 ± 0.36
42 m² g⁻¹). This difference was mainly partly attributed to enhanced photochemical formation of WI-
43 BrC species, such as oxygenated polycyclic aromatic hydrocarbons (OPAHs). In contrast, the
44 MACs of WS-BrC and WI-BrC were generally similar in winter and both showed little diel
45 differences. The Abs of wintertime WS-BrC correlated strongly with relative humidity, sulfate,
46 and NO₂, suggesting that aqueous-phase reactions is an important pathway for secondary BrC
47 formation during the winter season in Northwest China. Nitrophenols on average contributed
48 $2.44\pm 1.78\%$ of the Abs of WS-BrC in winter, but only $0.12\pm 0.03\%$ in summer due to faster
49 photodegradation reactions. WS-BrC and WI-BrC were estimated to account for $0.83\pm 0.23\%$ and
50 $0.53\pm 0.33\%$, respectively, of the total down-welling solar radiation in the UV range in summer,
51 and $1.67\pm 0.72\%$ and $2.07\pm 1.24\%$, respectively, in winter. The total absorption by BrC in the UV
52 region was about 55-79% relative to the elemental carbon (EC) absorption.

53 Keywords: Brown Carbon (BrC); Organic Aerosol; Optical Property; Molecular Composition

54

55 **1. Introduction**

56 Light-absorbing organic matter, termed as “brown carbon (BrC)”, has been recognized as an
57 important climate forcer due to its ability to directly interact with both incoming solar radiation
58 and outgoing terrestrial radiation (Andreae and Gelencser, 2006;Laskin et al., 2015). BrC is a
59 complex mixture of organic compounds, which collectively show a light absorption profile
60 increasing exponentially from the visible (Vis) to the ultraviolet (UV) range. Due to the high
61 abundance of organic aerosol in continental regions, especially in places with intensive
62 anthropogenic pollution, the contribution of BrC to aerosol absorption in the near-UV range is
63 potentially significant (Kirillova et al., 2014b;Huang et al., 2018;Yan et al., 2015a). For example,
64 a model study showed that BrC contributes up to $+0.25 \text{ W m}^{-2}$ of radiative forcing on a planetary
65 scale, which is approximately 19% of the absorption by anthropogenic aerosols (Feng et al., 2013).
66 Moreover, the strong absorption of BrC in the UV spectral region can reduce the solar actinic flux,
67 and subsequently affect atmospheric photochemistry and tropospheric ozone production (Jacobson,
68 1998;Mohr et al., 2013).

69 A thorough understanding of the sources and transformation processes of BrC in the
70 atmosphere is important, but it is still lacking. Biomass/biofuel combustion, including forest fires,
71 and burning of wood and agricultural wastes for residential cooking and heating, has been shown
72 as a particularly important source of BrC (Washenfelder et al., 2015;Desyaterik et al., 2013;Lin et
73 al., 2017). BrC can also be emitted directly from coal burning (Yan et al., 2017), and biogenic
74 release of fungi, plant debris, and humic matter (Rizzo et al., 2013;Rizzo et al., 2011). In addition,
75 recent studies suggested that secondary BrC can be formed through various reaction pathways,
76 including photooxidation of aromatic volatile organic compounds (VOCs) (Lin et al., 2015;Liu et

77 al., 2016), reactive uptake of isoprene epoxydiols onto preexisting sulfate aerosols (Lin et al.,
78 2014), aqueous oxidation of phenolic compounds and α -dicarbonyls (Chang and Thompson,
79 2010;Nozière and Esteve, 2005;Smith et al., 2016;Yu et al., 2014;Xu et al., 2018), and reactions
80 of ammonia or amines with carbonyl compounds in particles or cloud droplets (Nozière et al.,
81 2007;Laskin et al., 2010;Updyke et al., 2012;Nguyen et al., 2012;De Haan et al., 2018;Powelson
82 et al., 2014). However, atmospheric oxidation processes may also cause “photobleach” –
83 photodegradation of BrC into less light-absorbing compounds (Lee et al., 2014;Romonosky et al.,
84 2015;Sumlin et al., 2017), which may complicate the understanding of BrC in the atmosphere.

85 A common way to quantify the absorption properties of BrC is to measure the absorbance of
86 aerosol extracts over a wide wavelength range using spectrophotometers. This approach can
87 differentiate the interference of black carbon (BC) or mineral dust (Hecobian et al., 2010). Most
88 of the studies use ultrapure water to extract organic substance in the aerosol, and thus measure the
89 optical properties of water-soluble BrC (WS-BrC) (Wu et al., 2019;Hecobian et al., 2010;Kirillova
90 et al., 2014b). In addition, some studies analyzed the light absorption of BrC extracted using polar
91 organic solvents such as methanol or acetone (Liu et al., 2013;Huang et al., 2018;Kim et al., 2016).
92 Since such extracts contain both water-soluble and water-insoluble chromophores, little
93 information is available regarding the contribution and formation of water-insoluble BrC (WI-
94 BrC). However, it is important to understand WI-BrC given the facts that some water-insoluble
95 organic compounds, such as polycyclic aromatic hydrocarbons and their derivatives, are effective
96 light absorbers and that the mass absorption of WI-BrC could be even greater than that of the
97 water-soluble fraction (Chen and Bond, 2010;Huang et al., 2018;Sengupta et al., 2018). Thus, it is
98 necessary to extract water-soluble and water-insoluble organic components separately, e.g., via

99 using solvents with different polarity in sequence. Combining with measurements of BrC
100 molecular compositions, the UV-vis absorption properties of the water-soluble and water-insoluble
101 extracts may help us better understand the sources and formation mechanisms of light-absorbing
102 compounds in the atmosphere.

103 China has been experiencing serious atmospheric pollution conditions in recent decades, and
104 both model and field results showed elevated light absorption of BrC in most regions of China
105 (Huang et al., 2018; Cheng et al., 2011; Yan et al., 2017; Li et al., 2016b) compared to developed
106 countries such as the U.S. (Hecobian et al., 2010; Washenfelder et al., 2015) and European
107 countries (Mohr et al., 2013; Teich et al., 2017). However, BrC-related data are scarce in the
108 Guanzhong Basin (Shen et al., 2017; Huang et al., 2018), which is one of the most polluted regions
109 in China (van Donkelaar et al., 2010). Here we present measurements of the optical properties of
110 WS-BrC and WI-BrC in PM_{2.5} collected from a rural area of the Guanzhong Basin during winter
111 and summer seasons. We also measured the concentrations of several BrC compounds as well as
112 those of organic carbon (OC), elemental carbon (EC), water-soluble OC (WSOC) and inorganic
113 ions. These data were analyzed to examine the effects of sources emissions, daytime
114 photochemical oxidation, and aqueous-phase chemistry on WS- and WI-BrC components in
115 different seasons.

116 **2. Experimental section**

117 **2.1 Sample collection**

118 The sampling was conducted at a small village (namely Lincun, 34°44' N and 109°32' E, 354m
119 a.s.l.) ~ 40 km northeast to Xi'an, the capital of Shaanxi Province (Figure S1). The sampling site
120 is located in the central part of Guanzhong Basin with no obvious point source of air pollutants in

121 the surrounding areas. PM_{2.5} samples were collected twice a day (~8 am to ~~20~~8 pm and ~~~20~~~8 pm
122 to 8 am) onto prebaked (450 °C, 6-8 hr) quartz fiber filters (Whatman, QM-A, USA) during Aug.
123 3-23, 2016 and Jan. 20-Feb. 1, 2017 using a TISCH Environmental (USA) PM_{2.5} high volume
124 (1.13 m³ min⁻¹) sampler. Field blank samples were also collected by mounting blank filters onto
125 the sampler for about 15 min without pumping any air. After sampling, the sample filters were
126 immediately sealed in aluminum foil bags, and then stored in a freezer (-5 °C) prior to analysis.
127 Meteorological conditions, and concentrations of O₃ and NO₂ during this studied period are
128 presented in Figure 1.

129 **2.2 Filter extraction and absorption spectra analysis**

130 For each PM_{2.5} sample, a portion of the filter (~13.384 cm²) was first extracted in 8 ml of
131 Milli-Q water (18.2 MΩ) through 30 min of sonication at ~0°C. The water extract was then filtered
132 via vacuum filtration with a 25mm diameter 5 μm pore hydrophobic PTFE membrane filter (Merck
133 Millipore Ltd, MitexTM Membrane Filters, USA). Afterwards, the insoluble PM components
134 collected on the PTFE membrane filter and remained on the sample filter were rinsed with 2 ml
135 Milli-Q water, air dried, and then extracted via sonication in 8 ml pure acetonitrile (ACN)
136 (Honeywell Burdick & Jackson, LC/MS Grade, USA). The acetonitrile extract was filtered via a
137 13 mm diameter 0.45 μm pore syringe filter (PALL, Bulk Acrodisc®, PTFE Membrane Filters,
138 USA). The light absorption spectra of the water and the acetonitrile extracts were measured
139 between 190 nm to 820 nm by a diode-array spectrophotometer (Hewlett Packard 8452A, USA)
140 using quartz cuvettes with 1 cm length path. Field blank filters were extracted and measured in the
141 same manner as the samples. Data presented in this study were corrected for the field blanks (<10%
142 relative to field samples).

143 2.3 Chemical Analysis

144 OC and EC were analyzed using DRI Carbon Analyzer (Model 2001, USA). Another piece
145 of the filter sample (~8.6 cm²) was extracted with Milli-Q water (18.2MΩ), and filtered through
146 a PTFE syringe filter. Then the water-extract was analyzed for water-soluble inorganic ions
147 (SO₄²⁻, NO₃⁻, NH₄⁺, Cl⁻, F⁻, Ca²⁺, K⁺, Na⁺ and Mg²⁺) using a Metrohm Ion Chromatography
148 (Metrohm 940, Switzerland) and WSOC using a Shimadzu TOC analyzer (TOC-L CPH, Japan)
149 and. Concentrations of individual molecules, including levoglucosan, parent-PAHs, Oxygenated-
150 PAHs (OPAHs), nitrophenols, ~~and~~ isoprene and α-/β-pinene derived products, were measured
151 using GC/EI-MS (Agilent 7890A-5975C, USA) calibrated by authentic standards. More details
152 on these measurements can be found in previous publications (Li et al., 2014).

153 2.4 Data Interpretation

154 In this study, water-insoluble OC (WIOC) was calculated by the difference between OC and
155 WSOC:

$$156 M_{WIOC} = M_{OC} - M_{WSOC} \quad (1)$$

157 where M_{WIOC}, M_{OC}, and M_{WSOC} correspond to the mass concentration (in μgC m⁻³) of WIOC,
158 OC, and WSOC, respectively, in the air.

159 The absorption coefficient of WS-BrC (Abs_{λ,WS-BrC}, Mm⁻¹) or WI-BrC (Abs_{λ,WI-BrC}, Mm⁻¹)
160 at a given wavelength (λ) is determined from the UV-vis spectrum of the water extract (Hecobian
161 et al., 2010;Laskin et al., 2015)

$$162 Abs_{\lambda} = (A_{\lambda} - A_{700}) \times \frac{V_{solvent}}{V_a \times l} \times \ln(10) \times 100 \quad (2)$$

163 where A_λ is the absorbance of the water (A_{λ,WS-BrC}) or ACN (A_{λ,WI-BrC}) extract at λ, which is
164 corrected for the field blank, V_{solvent} (ml) is the volume of solvent (water or ACN) used to

165 extract the filter (8 mL), and V_a (m^3) is the air volume passed through the filter punch. l (cm) is
166 the optical length of the quartz cuvettes used for UV-vis measurement and $\ln(10)$ is used to
167 convert the logbase-10 (provided by the spectrophotometer) to natural logarithm. 100 is for unit
168 conversion. A_{700} (absorbance at the wavelength of 700 nm) is subtracted to minimize the
169 interference of baseline shift. The mass absorption coefficient of WS-BrC ($MAC_{\lambda,WS-BrC}$, $m^2 g^{-1}$)
170 or WI-BrC ($MAC_{\lambda,WI-BrC}$, $m^2 g^{-1}$) at wavelength of λ is calculated using eq (3)

$$171 \quad MAC_{\lambda} = \frac{Abs_{\lambda}}{M} \quad (3)$$

172 where M is the mass concentration of WSOC or WIOC. Note that since it is possible that not all
173 the WI-BrC was extracted into ACN, the $Abs_{\lambda,WI-BrC}$ (estimated uncertainty is 32%) and $MAC_{\lambda,WI-}$
174 BrC (estimated uncertainty is 33%) reported in this study are likely the lower bound values.
175 Nevertheless, the underestimation is probably insignificant since Chen and Bond (Chen and
176 Bond, 2010) reported that >92% of BrC was extractable by organic solvents (methanol or
177 acetone).

178 The wavelength dependence for BrC absorption is fit with a power law equation:

$$179 \quad Abs_{\lambda} = K \times \lambda^{-AAE} \quad (4)$$

180 where K is a constant and AAE stands for absorption Ångström exponent. In this study, the AAE
181 for a given sample is calculated through the linear regression of $\log(Abs_{\lambda})$ against $\log \lambda$ between
182 300–450 nm. This wavelength range is chosen because the fits of all the samples in this study are
183 better than $r^2=0.99$. Note that slightly higher AAE values (by up to 10%) are obtained using a
184 wider wavelength range (e.g., 300-550 nm; Figure S2).

185 The fraction of solar irradiance absorbed by particulate BrC at a given wavelength λ is
186 estimated following the Beer–Lambert’s law:

187
$$\frac{I_0 - I}{I_0}(\lambda) = 1 - e^{-b_{ap,\lambda,x} \times h_{ABL}} \quad (5)$$

188 where x denotes WS-BrC or WI-BrC, h_{ABL} is the atmospheric boundary layer height (assuming

189 1200 m in summer and 600 m in winter) according to the assumption that the ground

190 measurement results are representative of the average values in the whole planetary atmospheric

191 boundary layer (ABLPBL) (Kirchstetter et al., 2004; Kirillova et al., 2014a), (Kirchstetter et al.,

192 2004; Kirillova et al., 2014a). I_0 denotes the incident solar radiance in the form of either actinic

193 flux (in quanta $s^{-1} cm^{-2} nm^{-1}$) or irradiance (in $W m^{-2} nm^{-1}$), which were obtained using the TUV

194 Quick Calculator (http://cprm.acom.ucar.edu/Models/TUV/Interactive_TUV/). ($I_0 - I$) denotes the

195 direct absorption of solar actinic flux or irradiance by BrC, and $b_{ap,\lambda,x}$ corresponds to the

196 absorption coefficient (b_{ap} , m^{-1}) of WS-BrC or WI-BrC at wavelength of λ . The absorption

197 properties of BrC extracted by bulk solution may not entirely reflect the light absorption by

198 ambient aerosols. However, an estimated conversion factor can be calculated from the light

199 absorption of size-resolved samples using the Mie theory. Assuming that particles are of

200 spherical morphology and externally mixed with other light-absorbing components, an imaginary

201 refractive index (k , responsible for absorption) could be obtained from MAC using follow

202 equation (Laskin et al., 2015):

203
$$k_{(\lambda)} = \frac{\rho \times \lambda \times Abs_{\lambda}}{4\pi \times M_{WSOC}} = \frac{\rho \times \lambda \times MAC_{\lambda}}{4\pi} \quad (6)$$

204 where ρ (g/cm^3) was particle density and assigned as 1.5, and more details about Mie theory

205 calculations can be referred to the study by Liu et al. (2013). Previous studies showed that the light

206 absorption coefficient of particulate BrC ($b_{ap,\lambda,BrC}$) is around 0.7–2.0 times of that from bulk

207 solution ($Abs_{\lambda,WS-BrC}$ or $WI-BrC$) (Liu et al., 2013; Sun et al., 2007). Here, a conversion factor of 1.3

208 is applied based on a Mie theory calculation of aerosols in Xi'an (~ 40 km away from the sampling

209 site) (Wu, 2018). ~~I_0 denotes the incident solar radiance in the form of either actinic flux (in quanta~~
210 ~~$s^{-1}cm^{-2}nm^{-1}$) or irradiance (in $W m^{-2}nm^{-1}$), which were obtained using the TUV Quick Calculator~~
211 ~~(http://cprm.acom.ucar.edu/Models/TUV/Interactive_TUV/).~~ ~~$(I_0 - I)$ denotes the direct absorption~~
212 ~~of solar actinic flux or irradiance by BrC.~~

213 3. Results and Discussion

214 3.1 Optical absorption characteristics of WS-BrC and WI-BrC

215 The average absorption spectra of WS-BrC and WI-BrC ($\lambda = 300-700$ nm) during daytime
216 and nighttime in different seasons are shown in Figure 2a &b. The absorption Ångström
217 exponents for both WS-BrC (AAE_{WS-BrC}) and WI-BrC (AAE_{WI-BrC}) are generally higher than 5,
218 verifying the contribution of BrC to aerosol absorptivity in the region. The average AAE_{WS-BrC}
219 are similar between summer (5.43 ± 0.41) and winter (5.11 ± 0.53). Huang et al. (2014) and Shen et
220 al. (2017) reported comparable AAE_{WS-BrC} values (5.3-5.7) with no significant seasonal change
221 at urban sites of Xi'an, suggesting common characteristics of BrC on a regional scale in the
222 Guanzhong Basin of China. These results are comparable with the data reported in Guangzhou
223 (5.3) (Liu et al., 2018), but much lower than those in Beijing (5.3-7.3) (Cheng et al., 2011; Yan et
224 al., 2015b; Du et al., 2014) and Nanjing (6.7-7.3) (Chen et al., 2018). Moreover, Comparable
225 comparable AAE values were reported for WS-BrC in Switzerland (3.8-5.1) (Moschos et al.,
226 2018) and Nepal (4.2-5.6) (Wu et al., 2019; Kirillova et al., 2016), but higher AAE_{WS-BrC} were
227 found in Southeastern-southeastern US (7 ± 1) (Hecobian et al., 2010), Los Angeles Basin ($7.6 \pm$
228 0.5) (Zhang et al., 2013), and Korea (5.84-9.17) (Kim et al., 2016), and Beijing (7.0-7.5) (Cheng
229 et al., 2011).

230 The AAE_{WI-BrC} shows more obvious seasonal variations with a higher average value in

231 winter (6.04 ± 0.22) than in summer (5.01 ± 0.58). This difference suggests that the chemical
232 composition of WI-BrC might be more different in different seasons, due to variations in the
233 sources and atmospheric formation and aging processes of light absorbing hydrophobic
234 compounds.

235 The light absorption properties of WS-BrC and WI-BrC present obvious seasonal variations
236 (Figure 2). The average ($\pm 1\sigma$) Abs and MAC values of BrC at 365 nm (i.e., $\text{Abs}_{365, \text{WS-BrC}}$,
237 $\text{Abs}_{365, \text{WI-BrC}}$, $\text{MAC}_{365, \text{WS-BrC}}$, and $\text{MAC}_{365, \text{WI-BrC}}$) during daytime and nighttime in winter and
238 summer are summarized in Table 1. 365 nm ~~is was~~ chosen to avoid interferences from inorganic
239 compounds (e.g., nitrate and nitrite) and to be ~~consistence~~ consistent with previous studies
240 (Hecobian et al., 2010; Huang et al., 2018). On average, $\text{Abs}_{365, \text{WS-BrC}}$ is significantly higher than
241 $\text{Abs}_{365, \text{WI-BrC}}$ in summer ($5.00 \pm 1.28 \text{ Mm}^{-1}$ vs. $2.95 \pm 1.94 \text{ Mm}^{-1}$), but the values ~~are~~
242 comparable vary slightly in winter ($19.6 \pm 8.3 \text{ Mm}^{-1}$ vs. $21.9 \pm 13.5 \text{ Mm}^{-1}$). The substantially higher
243 BrC absorptions in winter correspond to a much higher organic aerosol concentration – WSOC
244 and WIOC concentrations in winter are on average 4.2 and 14 times of the concentrations in
245 summer (Table 1). Elevated OA (organic aerosols) concentration during winter is due to a
246 combination of lower ~~ABL-PBL~~ height and enhanced primary emissions (e.g., from residential
247 heating) in the cold season. It is worth noting that the wavelength-dependent Abs of WS-BrC
248 shows a minor tip at about 360 nm in both seasons (Figure 2), which may be related to the
249 contribution of some specific chromophores. For example, Lin et al. (2015) reported that some
250 nitrogen-containing organic compounds (such as picric acid or nitrophenol) have a maximum
251 absorption at wavelength of ~ 360 nm. The tip would possibly caused an overestimation of
252 average Abs and MAC at wavelength of 365 nm in this study. However, the influence seems

253 insignificant based on a comparison of average Abs and MAC at wavelength of 340 nm, 350 nm,
254 360 nm, 370 nm, and 380 nm (Table S1).–

255 The MACs of WS-BrC are comparable between the two seasons (Figure 2c & d), with the
256 average $\text{MAC}_{365, \text{WS-BrC}}$ being $1.00 (\pm 0.18) \text{ m}^2 \text{ g}^{-1}$ in summer and $0.93 (\pm 0.25) \text{ m}^2 \text{ g}^{-1}$ in winter
257 (Table 1). As summarized in Table 2, the $\text{MAC}_{365, \text{WS-BrC}}$ measured in this study, i.e., at a rural
258 site in the Guanzhong Basin of China, is comparable to or lower than the values observed in
259 Asian cities such Xi'an (Huang et al., 2018), Beijing (Cheng et al., 2011), Seoul (Kim et al.,
260 2016) and New Delhi (Kirillova et al., 2014b), but obviously higher than those in the regional
261 sites of North China Plain (Teich et al., 2017) and the background site of Tibetan Plateau (Xu et
262 al., 2020). ~~However~~ Moreover, significantly lower $\text{MAC}_{365, \text{WS-BrC}}$ values were observed in the
263 US, including Los Angeles Basin (Zhang et al., 2013), Southeastern US (Hecobian et al., 2010),
264 and Atlanta (Liu et al., 2013).

265 In winter, the average $\text{MAC}_{365, \text{WI-BrC}}$ ($0.95 \pm 0.32 \text{ m}^2 \text{ g}^{-1}$) is comparable to $\text{MAC}_{365, \text{WS-BrC}}$
266 ($0.93 \pm 0.25 \text{ m}^2 \text{ g}^{-1}$; Table 1). However, in summer the $\text{MAC}_{365, \text{WI-BrC}}$ is significantly much higher
267 than $\text{MAC}_{365, \text{WS-BrC}}$ (1.82 ± 1.06 vs. $1.00 \pm 0.18 \text{ m}^2 \text{ g}^{-1}$), indicating a relatively stronger light
268 absorption capability of hydrophobic chromophores than hydrophilic chromophores. Further, the
269 fact that the summertime $\text{MAC}_{365, \text{WI-BrC}}$ is nearly double the wintertime $\text{MAC}_{365, \text{WI-BrC}}$ suggests
270 that more light absorbing molecules are formed in the warm season.

271 Figure 2 compares the wavelength-dependent light absorptivity (i.e., Abs_λ and MAC_λ) of
272 WS-BrC and WI-BrC between day and night in summer and winter. Higher $\text{Abs}_{\lambda, \text{WS-BrC}}$ and
273 $\text{Abs}_{\lambda, \text{WI-BrC}}$ occurred during daytime in summer but during nighttime in winter. The MAC_λ of
274 WS-BrC are overall similar between daytime and nighttime in both seasons. However, the MAC_λ

275 of WI-BrC show a significant daytime increase in summer over the whole wavelength range of
276 300-700 nm (Figure 2c). The day-night change of BrC light absorptivity can be viewed more
277 obviously in Figure 1e and 1f, where the temporal variations of the Abs_{365} and MAC_{365} of WS-
278 BrC and WI-BrC during summer 2016 (Aug. 3-23) and winter 2017 (Jan. 20 -Feb. 1) are
279 presented. The highest day/night ratio of $MAC_{365,WIOC}$ reached 3.8 in summer and the average
280 daytime $MAC_{365,WI-BrC}$ in summer ($2.45 \pm 1.14 \text{ m}^2 \text{ g}^{-1}$) is more than twice the value during
281 nighttime ($1.18 \pm 0.36 \text{ m}^2 \text{ g}^{-1}$; Table 1). A possible reason for this observation is that there are
282 additional sources of WI-BrC during summer daytime in this rural region, such as secondary
283 formation of hydrophobic light absorbing compounds.

284 Figure 3 and 4 present the cross-correlations of $Abs_{365,WS-BrC}$ and $Abs_{365,WI-BrC}$ with major
285 chemical components (e.g., WSOC, WSIC, and sulfate) and molecular tracer species in summer
286 and winter, respectively. In winter, $Abs_{365,WS-BrC}$ correlates strongly with WSOC concentration
287 ($r^2=0.80$), so does $Abs_{365,WI-BrC}$ with WIOC ($r^2=0.76$). However, their relationships in summer are
288 much weaker, especially for the correlation between $Abs_{365,WI-BrC}$ and WIOC ($r^2=0.50$).
289 Considering that secondary OA (SOA) are mainly comprised of water-soluble compounds, such
290 as polyalcohols/polyacids and phenols (Kondo et al., 2007), the much higher WSOC/OC ratio in
291 summer (0.75 ± 0.07) compared to winter (0.50 ± 0.09) confirms more prevalent SOA formation in
292 summer associated with higher ~~air~~ temperature and stronger solar radiation. Formation of
293 secondary organic chromophores may lead to a more complex composition of BrC in summer.
294 More evidences on secondary BrC formation are provided in the subsequent sections.

295 Numerous studies reported that biomass burning is a dominant source of BrC in the
296 atmosphere (Desyaterik et al., 2013; Washenfelder et al., 2015). In the current study,

297 levoglucosan – a key tracer for biomass burning emissions (Simoneit, 2002) – was determined.
298 As shown in Figure 3 and 4, levoglucosan correlates well with WSOC and WIOC in both
299 summer and winter ($r^2=0.45-0.77$), suggesting that biomass burning is an important source of OA
300 in the rural region of Guanzhong Basin. For most of the periods in this study, the $MAC_{365,WS-BrC}$
301 and $MAC_{365,WI-BrC}$ values are within the range of MAC of biomass burning aerosols (e.g.,
302 1.3–1.8 for corn stalk (Li et al., 2016a), ≈ 1.37 for rice straw (Park and Yu, 2016), ~ 1.9 for BB
303 smoke particles (Lin et al., 2017)). Also, $Abs_{365,WI-BrC}$ in both summer and winter correlate well
304 with levoglucosan ($r^2=0.74$ and 0.62 , respectively), demonstrating an important contribution of
305 biomass burning to WI-BrC despite the fact that levoglucosan itself is water soluble. The
306 relationships between the $Abs_{365,WS-BrC}$ and levoglucosan are much weaker ($r^2=0.40$ and 0.45 in
307 summer and winter, respectively), suggesting more complex sources of WS-BrC in the region.

308 **3.2 Molecular characterization of BrC aerosols**

309 Five categories of molecular tracer compounds, i.e., parent-polycyclic aromatic
310 hydrocarbons (parent-PAHs), oxygenated-PAHs (OPAHs), nitrophenols, isoprene-derived
311 products (SOA_i), and α -/ β -pinene-derived products (SOA_p), were determined by the GC-EIMS
312 technique to investigate the formation pathways of BrC in this study. Their average
313 concentrations as well as daytime and nighttime differences are summarized in Table 1, and the
314 temporal variation profiles of the sum concentrations of each category, together with
315 levoglucosan time series, are presented in Figure S3.

316 PAHs and their derived-oxidized productseompounds are important BrC chromophores,
317 since the large conjugated polycyclic structures are strongly light-absorbing in the near-UV
318 range (Samburova et al., 2016;Huang et al., 2018). A total number of 14 parent PAHs and 5

319 OPAHs (Table S4S2) were determined in this study. Parent-PAHs are unsubstituted PAHs
320 mainly emitted directly from incomplete combustions of coal, biofuel, gasoline or other materials
321 whereas OPAHs can be emitted directly from combustion sources or formed from photochemical
322 oxidation of the parent-PAHs. The time trends of parent-PAHs and OPAHs are highly similar in
323 both seasons ($r^2 = 0.90$ and 0.98 in summer and winter, respectively, Figure 3 and 4), suggesting
324 that they have common combustion sources. In addition, both parent-PAHs and OPAHs
325 presented good correlations with levoglucosan, particularly in winter ($r^2 = 0.69$ and 0.73 ,
326 respectively; Figure 4), indicating that ~~that~~ biomass burning is an important contributor to ~~air~~
327 ambient particulate PAHs in the region. PAHs, as well as levoglucosan, are elevated during
328 nighttime in winter, corresponding to enhanced biomass burning emissions from heating-related
329 activities as well as reduced boundary layer height at night. In contrast, the average daytime
330 concentrations of parent-PAHs ($11.6 \pm 5.7 \text{ ng m}^{-3}$) and levoglucosan ($142 \pm 89 \text{ ng m}^{-3}$) in summer
331 are about 1.95 and 2.58 times, respectively, of the values at night (Table 1). The daytime
332 enhancement of OPAHs concentrations in summer is even more pronounced with an average
333 day/night ratio of ~ 4.6 and as high as 9.8 for individual OPAH species (e.g., 6H-
334 benzo(cd)pyrene-6-one; Figure S4). Both parent-PAHs and OPAHs, which are hydrophobic thus
335 mainly exist as WIOC, demonstrate a good linear relationship with $\text{Abs}_{365, \text{WI-BrC}}$ in both winter
336 and summer ($r^2 = 0.49$ - 0.83 , Figure 3 and 3). However, the good correlation between OPAHs and
337 $\text{Abs}_{365, \text{WI-BrC}}$ in summer appears to be mainly driven by daytime production, as the correlation
338 coefficient (r^2) is 0.72 for the daytime data but is <0.1 for the nighttime data (Figure S5a). These
339 results suggest that photochemical formation of light-absorption compounds is an important
340 source of BrC during summer in the Guanzhong Basin.

341 We estimated the potential contribution of parent-PAHs and OPAHs to the light absorption
342 of WI-BrC using a method reported in Samburova et al. (2016). Details on the method are
343 presented in the Supplementary Information (SI). Table [S2-S3](#) summarizes the solar-spectrum-
344 weighed mass absorption coefficients for PAHs ($MAC_{PAH,av}$) used in the calculation. As shown
345 in Figure 5, the contribution of parent-PAHs to solar-spectrum-weighted absorption coefficient of
346 WI-BrC varies between 0.55% - 0.66% with slight diurnal or season variations (Table [S2S3](#)).
347 However, the contribution of OPAHs clearly shows higher daytime values, especially in
348 summer. The average contribution of OPAHs to the solar-spectrum-weighted absorption
349 coefficient of WI-BrC in summer is $0.51\pm 0.28\%$ during daytime and $0.34\pm 0.19\%$ during
350 nighttime. These results indicate that more secondary water-insoluble aromatic chromophores
351 were produced via photochemical oxidation during summertime in the rural region.

352 Nitrophenols were identified as one of the most important light-absorbing compounds in
353 particles and cloud water influenced by BB emission in China (Desyaterik et al., 2013). These
354 compounds can be either directly emitted from burning of biomass (Xie et al., 2019) or formed in
355 the atmosphere through gas phase and aqueous phase reactions of aromatic precursors including
356 benz[a]pyrene (Lu et al., 2011), naphthalene (Kitanovski et al., 2014), catechol and guaiacol
357 (Ofner et al., 2011), and toluene (Liu et al., 2015) in the presence of NO_x . In this study, only a
358 few nitrophenol compounds were detected in PM (Table [S1S2](#)) and their average ($\pm 1\sigma$)
359 concentration is $0.94 (\pm 0.26) \text{ ng m}^{-3}$ in summer and $72.6 (\pm 63.7) \text{ ng m}^{-3}$ in winter. The
360 wintertime concentrations of nitrophenols measured in the current study are comparable to those
361 detected in Shanghai (Li et al., 2016b), Mt. Tai in the Shandong province of China (Desyaterik et
362 al., 2013), and Ljubljana of Slovenia (Kitanovski et al., 2012), but the summertime

363 concentrations observed are more comparable to those detected in the Los Angeles Basin of the
364 U.S. (Zhang et al., 2013). The substantially lower concentration of nitrophenols in summer may
365 be related to rapid photodegradation in the atmosphere. Indeed, according to a laboratory study
366 conducted by Zhao et al. (2015) the timescale for photo-bleaching of nitrophenols can be an hour
367 or less. Furthermore, as shown in Figure S5b, during wintertime, when low temperature and
368 weak solar irradiation suppress photodegradation process, nitrophenols concentration anti-
369 correlates with O₃ mixing ratio in a nonlinear manner ($r^2=0.60$). On average, concentration of
370 nitrophenols in winter ~~present is~~ 2.5 times higher ~~concentration~~ during nighttime than during
371 daytime whereas the nighttime concentrations of levoglucosan and PAHs are only slightly higher
372 than the daytime concentrations (by 11% and 33%, respectively; Table 1). Levoglucosan and
373 PAHs are less photochemically reactive than nitrophenols. These results confirm that
374 nitrophenols, and other photoreactive BrC compounds, may undergo significant atmospheric
375 degradation during summertime.

376 Both summertime and wintertime Abs_{365,WS-BrC} correlated well with the concentrations of
377 nitrophenols ($r^2=0.51-0.72$, Figure S5c & d), suggesting an important contribution of nitrated
378 aromatic compounds to light absorption of WS-BrC in the study area. Using the MAC of
379 individual nitrophenol reported in Zhang et al. (2013), we calculated that the contributions of
380 nitrophenols to aerosol light absorption are 6.5-27 times higher than their mass contributions to
381 WSOC and that the fractions are much higher in winter ($2.44\pm 1.78\%$) than in summer
382 ($0.12\pm 0.03\%$; Table S3). In addition, due to a significantly higher abundance of nitrophenols
383 during nighttime in winter, their fractional contribution to aerosol absorption is on average 2.5
384 times higher than during the day ($3.47\pm 2.03\%$ vs. $1.41\pm 0.29\%$).

385 On a global scale, biogenic VOCs, mostly consisting of isoprene and monoterpenes, are
386 nearly an order of magnitude more abundant than anthropogenic VOCs (Guenther et al., 2006),
387 and their secondary products are estimated to be a predominant contributor to global SOA
388 burden (Heald et al., 2008). Recent studies (Lin et al., 2014; Nakayama et al., 2015; Nakayama et
389 al., 2012) showed that a large amount of biogenic SOA compounds are light absorptive. Some
390 tracers of SOA formed from isoprene (SOA_i) and α -/ β -pinene (SOA_p) oxidation were measured
391 in the summertime samples (Table S1S2), and their temporal variations are shown in Figure S3.
392 No biogenic SOA tracer species were detectable in the winter samples in this study. Similar
393 results were obtained in our previous study in the Mt. Hua of the Guanzhong Basin (Li, 2011).
394 These findings are consistent with low emissions of biogenic VOCs and low oxidation rates in
395 this region during cold seasons. The average concentrations of SOA_i and SOA_p tracers in
396 summer are 18.6 ± 9.7 and 22.0 ± 6.7 ng m⁻³, respectively. Neither SOA_i tracers nor SOA_p tracers
397 showed significant correlations with the absorption coefficient of WSOC or WSIC, suggesting a
398 low contribution of biogenic SOA to aerosol light absorption in the region. In addition, compared
399 to the MAC values observed in this study, the MACs of biogenic SOA reported in literature are
400 much lower, on average, by nearly an order of magnitude (Laskin et al., 2015), which further
401 support an insignificant contribution of biogenic sources to BrC in this region. This finding is
402 consistent with the fact that the Guanzhong Basin is a highly polluted region, where the major
403 emission sources of organic aerosols are anthropogenic.

404 3.3 Variation of BrC during extreme haze events in winter

405 In recent years, ~~extreme~~extremely severe haze events with very high PM_{2.5} concentrations
406 (up to 500-600 $\mu\text{g m}^{-3}$) and low visibility (lower than 1 km) occurred frequently during

407 wintertime in China (Huang et al., 2014). In this study, ~~a heavy and extreme~~ haze event occurred
408 during Jan. 21-26 when PM_{2.5} concentration at the rural site increased continuously from ~100
409 $\mu\text{g m}^{-3}$ to 430 $\mu\text{g m}^{-3}$ and visibility decreased from >10 km to ~1.4 km (Figure 1b & d). Similar
410 to most haze events occurred in Northeast China, this event was associated with stagnant
411 meteorological condition with low wind speed ($<1 \text{ km s}^{-1}$), which promotes the accumulation of
412 pollutants. In addition, secondary inorganic aerosol species, e.g., SO_4^{2-} , NO_3^- and NH_4^+ ,
413 increased sharply (Figure 1d), which indicates secondary aerosol formation was enhanced during
414 the haze event despite the low solar irradiance and low O₃ concentration (e.g., $2 \sim 40 \mu\text{g m}^{-3}$;
415 Figure 1c) conditions. Recent studies by Wang et al. (2016) and Cheng et al. (2016) reported
416 dramatic increases of secondary inorganic components, mainly sulfate, nitrate and ammonium
417 (SNA), during haze periods in China and attributed the increases to enhanced aqueous reactions
418 under high relative humidity (RH) conditions with NO₂ being an important oxidant. Moreover,
419 Huang et al. (2014) observed that SOA also increased obviously during haze periods in winter.
420 Indeed, as shown in Figure 4, SO_4^{2-} correlates well with RH ($r^2=0.64$) and NO₂ ($r^2=0.56$) in
421 winter. In addition, Abs_{365,WS-BrC}, which increases continuously during the haze period with a
422 peak value at 43.3 Mm⁻¹ (Figure 1e), correlates well with RH ($r^2=0.65$), sulfate ($r^2=0.84$) and
423 NO₂ ($r^2=0.70$) (Figure 4). In contrast, Abs_{365,WI-BrC} presents obvious diurnal variation during the
424 haze period, and the ~~relationship~~ correlations of RH ($r^2=0.40$), sulfate ($r^2=0.46$) and NO₂
425 ($r^2=0.41$) with Abs_{365,WI-BrC} are also much weaker than those with Abs_{365,WS-BrC}. These results
426 suggest that aqueous oxidation has played a role in the formation of WS-BrC (Laskin et al.,
427 2015) during the haze period, although the stagnant meteorological condition with low wind
428 speed can also promote its accumulation. This finding is consistent with our previous

429 ~~studies~~ study conducted in Xi'an (Wu et al., 2020), which ~~also found a secondary formation of~~
430 ~~BrC in winter by using stable carbon isotope composition analysis~~ have shown that aqueous-
431 ~~reactions can be an important pathway of BrC formation in the atmosphere (Laskin et al., 2015).~~
432 In contrast, a slowly decreasing trend of $MAC_{365,WIOC}$ ~~is~~ was observed during the haze period,
433 suggesting that some of the water-insoluble BrC species were oxidized to form water-soluble
434 chromophores, possibly through aqueous-phase reactions.

435 It is worthwhile to mention that Jan. 27, 2017 was the Chinese New Year's Eve and a large
436 amount of fireworks were set off for celebration. During this night, the concentrations of $PM_{2.5}$,
437 OC, EC, WSOC and WIOC as well as SNA were ~~actually~~ 25%-51% lower than their wintertime
438 average concentrations due to the higher wind speed favoring for atmospheric dispersion (Figure
439 1). However, ~~the~~ $MAC_{365,WS-BrC}$ (1.81) increased to about 2 times of its average value in
440 winter, ~~and~~ $Abs_{365,WS-BrC}$ ($20.5 Mm^{-1}$) also showed a slight increase. ~~while~~ OC, EC, WSOC
441 ~~and WIOC as well as SNA were actually 25%-51% lower than their wintertime average~~
442 ~~concentrations (Figure 1d).~~ Meanwhile, metal ions, which are abundant in fireworks (Wu et al.,
443 2018; Jiang et al., 2015), such as K^+ , Mg^{2+} , and Ca^{2+} , ~~increased~~ substantially during the night as
444 well (Figure S6). These results indicate that the increase of $MAC_{365,WSOC}$ during the Chinese
445 New Year's Eve is likely mainly contributed by metal-containing light-absorbing compounds
446 emitted from fireworks (Laskin et al., 2015; Tran et al., 2017).

447 **3.4 Estimation of direct absorption of solar radiation by BrC**

448 Since the light absorption of BrC is mainly in the UV spectral region, an important concern
449 is that BrC can reduce the solar actinic flux and thus affect atmospheric photochemistry and
450 tropospheric ozone production (Jacobson, 1998; Mohr et al., 2013). In this study, the direct

451 absorptions of solar radiation by both WS-BrC and WI-BrC ~~are-were~~ estimated by using Eq 7.
452 Figure S7 presents the incident solar irradiance and actinic flux spectra determined for the region
453 under midday summer (Aug. 10, 2016 13:00 pm Beijing (BJ) time) and winter (Jan. 25, 2017
454 13:00 pm BJ time) conditions. Note that the local time at Guanzhong is ~ 1 hour later than the BJ
455 time.

456 Table 3 presents a summary of the calculated direct solar absorptions of BrC. In summer,
457 the direct attenuation of actinic flux by WS-BrC and WI-BrC are estimated at
458 $1.55 \times 10^{14} \pm 0.43 \times 10^{14}$ and $1.03 \times 10^{14} \pm 0.64 \times 10^{14}$ quanta $s^{-1} cm^{-2}$, respectively, in the UV range
459 (300-400 nm), which account for $0.83 \pm 0.23\%$ and $0.53 \pm 0.33\%$, respectively, of the total down-
460 welling radiation. In winter, the direct absorptions by BrC are higher with WS-BrC and WI-BrC
461 on average accounting for $1.67 \pm 0.72\%$ and $2.07 \pm 1.24\%$, respectively, of the total down-welling
462 radiation in the UV range. These results suggest that BrC may have a significant influence on
463 atmospheric photochemistry in the UV range. In the visible spectral region (400 - 700 nm), the
464 contributions of WS-BrC and WI-BrC to the total down-welling radiation are negligible –
465 $0.10 \pm 0.03\%$ and $0.07 \pm 0.05\%$ in summer, and $0.15 \pm 0.06\%$ and $0.15 \pm 0.08\%$ in winter,
466 respectively.

467 Another concern of BrC is that they can absorb solar irradiance to influence tropospheric
468 temperature in a similar way as black carbon (BC) or elemental carbon (EC) (Feng et al.,
469 2013;Laskin et al., 2015). In our study, the direct absorption of solar irradiance by WS-BrC and
470 WI-BrC are estimated at 0.51 ± 0.14 and 0.34 ± 0.21 $W m^{-2}$ in summer, and 0.57 ± 0.25 and
471 0.68 ± 0.41 $W m^{-2}$ in winter in the UV range. To evaluate the contribution of BrC to total aerosol
472 absorption, we also estimated the direct absorption of EC based on the Carbon Analyzer data

473 according to the method described by Kirillova et al. (2014b) and Kirchstetter and Thatcher
474 (2012) (see SI). The estimated contributions of light absorption of BrC relative to EC are shown
475 in Table 3. In the visible region, the contribution is estimated at $10.0 \pm 3.52\%$ in summer and
476 $4.99 \pm 1.23\%$ in winter for WS-BrC, and $6.19 \pm 2.42\%$ and $4.51 \pm 1.44\%$, respectively, for WI-BrC.
477 However, in the UV range, the fractions increase to $49.3 \pm 14.5\%$ in summer and $25.9 \pm 5.47\%$ in
478 winter for WS-BrC, $29.4 \pm 11.0\%$ and $29.0 \pm 10.4\%$ for WI-BrC, which are within the range of the
479 values reported in other regions in China (Huang et al., 2018), India (Kirillova et al., 2014b), and
480 Korea (Kirillova et al., 2014a). On the other hand, the direct light absorption of WI-BrC
481 represents a substantive contribution to that of total BrC in this study, which is about 40% in
482 summer and more than 50% in winter in both UV and visible range, emphasizing the important
483 role that WI-BrC likely plays in atmospheric chemistry and the Earth's climate system,
484 especially in China.

485 **4. Summary and Conclusion**

486 Both WS-BrC and WI-BrC showed elevated Abs in winter (4-7 times higher than those in
487 summer), corresponding to much higher concentrations of WSOC and WIOC due to a
488 combination of lower ABL/PBL height and enhanced primary emissions (e.g., from residential
489 heating) in the cold season. No significant differences were found for the daytime and nighttime
490 MACs of WS-BrC in summer, or for the MACs of WS-BrC and WI-BrC in winter. However, the
491 average daytime $MAC_{365, WI-BrC}$ was more than twice the nighttime value in summer. We found
492 that the average daytime concentrations of both parent-PAHs and levoglucosan in summer were
493 around 2 times of the values at night and the daytime OPAHs concentration was more than 4
494 times of the nighttime value. Moreover, OPAHs and well correlated with $Abs_{365, WI-BrC}$ in summer

495 ~~correlated well~~ during daytime ($r^2=0.72$) ~~in summer~~ but not during nighttime ($r^2<0.1$). These
496 results demonstrated that photochemical formation of BrC and enhanced BB emissions (e.g.,
497 from cooking) contributed to the higher daytime MACs in summer. In winter, the Abs of WS-
498 BrC correlated strongly with relative humidity, sulfate, and NO_2 , suggesting that aqueous-phase
499 reactions played an important role in the formation of secondary BrC. $\text{Abs}_{365, \text{WS-BrC}}$ correlated
500 well with the concentrations of nitrophenols in both seasons, suggesting an important
501 contribution of nitrated aromatic compounds to light absorption of WS-BrC. However, this
502 contribution is much lower in summer due to faster photodegradation reactions of these
503 compounds. WS-BrC and WI-BrC were estimated to account for $0.83\pm 0.23\%$ and $0.53\pm 0.33\%$,
504 respectively, of the total down-welling solar radiation in the UV range in summer, and
505 $1.67\pm 0.72\%$ and $2.07\pm 1.24\%$, respectively, in winter. The substantive contribution of WI-BrC to
506 total BrC absorption ($\sim 40\%$ in summer and $>50\%$ in winter) emphasize the important role that
507 WI-BrC likely plays in atmospheric chemistry and the Earth's climate system.

508

509

510

511 **Author Contributions**

512 J.J. Li, Q. Zhang, G.H. Wang, K.F. Ho, and J.J. Cao designed the experiment. J.J. Li, G.H. Wang,
513 and K.F. Ho arranged the sample collection. J. Li, L. Liu and C. Wu collected the samples. J.J.
514 Li, J. Li, J.Y. Wang, W.Q. Jiang, and L.J. Li analyzed the samples. J.J. Li, Q. Zhang, and G.H.
515 Wang performed the data interpretation. J.J. Li, Q. Zhang, and G.H. Wang wrote the paper.

516

517 **Acknowledgements**

518 This work was financially supported by the program from National Nature Science Foundation
519 of China (No. 41773117, 91644102, 41977332, 91543116). [Jianjun Li also acknowledged the](#)
520 [support of the Youth Innovation Promotion Association CAS \(No. 2020407\)](#). The authors

521 gratefully acknowledge National Center for Atmospheric Research for the provision of the solar
522 actinic flux and irradiance data (TUV Quick Calculator,
523 http://cprm.acom.ucar.edu/Models/TUV/Interactive_TUV/) used in this publication.

524

525

526 **References**

- 527 Andreae, M. O., and Gelencser, A.: Black carbon or brown carbon? The nature of light-absorbing carbonaceous
528 aerosols, *Atmos. Chem. Phys.*, 6, 3131-3148, 10.5194/acp-6-3131-2006, 2006.
- 529 Chang, J. L., and Thompson, J. E.: Characterization of colored products formed during irradiation of aqueous
530 solutions containing H₂O₂ and phenolic compounds, *Atmos. Environ.*, 44, 541-551,
531 10.1016/j.atmosenv.2009.10.042, 2010.
- 532 Chen, Y., and Bond, T. C.: Light absorption by organic carbon from wood combustion, *Atmos. Chem. Phys.*, 10,
533 1773-1787, 10.5194/acp-10-1773-2010, 2010.
- 534 Chen, Y., Ge, X., Chen, H., Xie, X., Chen, Y., Wang, J., Ye, Z., Bao, M., Zhang, Y., and Chen, M.: Seasonal light
535 absorption properties of water-soluble brown carbon in atmospheric fine particles in Nanjing, China, *Atmos.*
536 *Environ.*, 187, 230-240, 10.1016/j.atmosenv.2018.06.002, 2018.
- 537 Cheng, Y., He, K. B., Zheng, M., Duan, F. K., Du, Z. Y., Ma, Y. L., Tan, J. H., Yang, F. M., Liu, J. M., Zhang, X. L.,
538 Weber, R. J., Bergin, M. H., and Russell, A. G.: Mass absorption efficiency of elemental carbon and water-
539 soluble organic carbon in Beijing, China, *Atmos. Chem. Phys.*, 11, 11497-11510, 10.5194/acp-11-11497-2011,
540 2011.
- 541 Cheng, Y., Zheng, G., Wei, C., Mu, Q., Zheng, B., Wang, Z., Gao, M., Zhang, Q., He, K., Carmichael, G., Pöschl,
542 U., and Su, H.: Reactive nitrogen chemistry in aerosol water as a source of sulfate during haze events in China,
543 *Science Advances*, 2, 10.1126/sciadv.1601530, 10.1126/sciadv.1601530, 2016.
- 544 De Haan, D. O., Tapavicza, E., Riva, M., Cui, T. Q., Surratt, J. D., Smith, A. C., Jordan, M. C., Nilakantan, S.,
545 Almodovar, M., Stewart, T. N., de Loera, A., De Haan, A. C., Cazaunau, M., Gratien, A., Pangu, E., and
546 Doussin, J. F.: Nitrogen-Containing, Light-Absorbing Oligomers Produced in Aerosol Particles Exposed to
547 Methylglyoxal, Photolysis, and Cloud Cycling, *Environ. Sci. Technol.*, 52, 4061-4071,
548 10.1021/acs.est.7b06105, 2018.
- 549 Desyaterik, Y., Sun, Y., Shen, X., Lee, T., Wang, X., Wang, T., and Collett Jr., J. L.: Speciation of “brown” carbon in
550 cloud water impacted by agricultural biomass burning in eastern China, *J. Geophys. Res.-Atmos.*, 118, 7389-
551 7399, doi:10.1002/jgrd.50561, 2013.
- 552 Du, Z., He, K., Cheng, Y., Duan, F., Ma, Y., Liu, J., Zhang, X., Zheng, M., and Weber, R.: A yearlong study of water-
553 soluble organic carbon in Beijing II: Light absorption properties, *Atmos. Environ.*, 89, 235-241,
554 10.1016/j.atmosenv.2014.02.022, 2014.
- 555 Feng, Y., Ramanathan, V., and Kotamarthi, V. R.: Brown carbon: a significant atmospheric absorber of solar
556 radiation?, *Atmos. Chem. Phys.*, 13, 8607-8621, 10.5194/acp-13-8607-2013, 2013.
- 557 Guenther, A., Karl, T., Harley, P., Wiedinmyer, C., Palmer, P. I., and Geron, C.: Estimates of global terrestrial
558 isoprene emissions using MEGAN (Model of Emissions of Gases and Aerosols from Nature), *Atmos. Chem.*
559 *Phys.*, 6, 3181-3210, 2006.
- 560 Heald, C. L., Henze, D. K., Horowitz, L. W., Feddema, J., Lamarque, J. F., Guenther, A., Hess, P. G., Vitt, F.,
561 Seinfeld, J. H., Goldstein, A. H., and Fung, I.: Predicted change in global secondary organic aerosol

562 concentrations in response to future climate, emissions, and land use change, *J. Geophys. Res.-Atmos.*, 113,
563 doi: 10.1029/2007jd009092, 10.1029/2007jd009092, 2008.

564 Hecobian, A., Zhang, X., Zheng, M., Frank, N., Edgerton, E. S., and Weber, R. J.: Water-Soluble Organic Aerosol
565 material and the light-absorption characteristics of aqueous extracts measured over the Southeastern United
566 States, *Atmos. Chem. Phys.*, 10, 5965-5977, 10.5194/acp-10-5965-2010, 2010.

567 Huang, R.-J., Zhang, Y., Bozzetti, C., Ho, K.-F., Cao, J.-J., Han, Y., Daellenbach, K. R., Slowik, J. G., Platt, S. M.,
568 Canonaco, F., Zotter, P., Wolf, R., Pieber, S. M., Bruns, E. A., Crippa, M., Ciarelli, G., Piazzalunga, A.,
569 Schwikowski, M., Abbaszade, G., Schnelle-Kreis, J., Zimmermann, R., An, Z., Szidat, S., Baltensperger, U., El
570 Haddad, I., and Prevot, A. S. H.: High secondary aerosol contribution to particulate pollution during haze
571 events in China, *Nature*, 514, 218-222, 10.1038/nature13774, 2014.

572 Huang, R.-J., Yang, L., Cao, J., Chen, Y., Chen, Q., Li, Y., Duan, J., Zhu, C., Dai, W., Wang, K., Lin, C., Ni, H.,
573 Corbin, J. C., Wu, Y., Zhang, R., Tie, X., Hoffmann, T., O'Dowd, C., and Dusek, U.: Brown Carbon Aerosol in
574 Urban Xi'an, Northwest China: The Composition and Light Absorption Properties, *Environ. Sci. Technol.*, 52,
575 6825-6833, 10.1021/acs.est.8b02386, 2018.

576 Jacobson, M. Z.: Studying the effects of aerosols on vertical photolysis rate coefficient and temperature profiles over
577 an urban airshed, *J. Geophys. Res.-Atmos.*, 103, 10593-10604, 10.1029/98jd00287, 1998.

578 Jiang, Q., Sun, Y. L., Wang, Z., and Yin, Y.: Aerosol composition and sources during the Chinese Spring Festival:
579 fireworks, secondary aerosol, and holiday effects, *Atmos. Chem. Phys.*, 15, 6023-6034, 10.5194/acp-15-6023-
580 2015, 2015.

581 Kim, H., Kim, J. Y., Jin, H. C., Lee, J. Y., and Lee, S. P.: Seasonal variations in the light-absorbing properties of
582 water-soluble and insoluble organic aerosols in Seoul, Korea, *Atmos. Environ.*, 129, 234-242,
583 <https://doi.org/10.1016/j.atmosenv.2016.01.042>, 2016.

584 Kirchstetter, T. W., Novakov, T., and Hobbs, P. V.: Evidence that the spectral dependence of light absorption by
585 aerosols is affected by organic carbon, *J. Geophys. Res.-Atmos.*, 109, doi:10.1029/2004JD004999,
586 10.1029/2004jd004999, 2004.

587 Kirchstetter, T. W., and Thatcher, T. L.: Contribution of organic carbon to wood smoke particulate matter absorption
588 of solar radiation, *Atmos. Chem. Phys.*, 12, 6067-6072, 10.5194/acp-12-6067-2012, 2012.

589 Kirillova, E. N., Andersson, A., Han, J., Lee, M., and Gustafsson, Ö.: Sources and light absorption of water-soluble
590 organic carbon aerosols in the outflow from northern China, *Atmos. Chem. Phys.*, 14, 1413-1422, 10.5194/acp-
591 14-1413-2014, 2014a.

592 Kirillova, E. N., Andersson, A., Tiwari, S., Srivastava, A. K., Bisht, D. S., and Gustafsson, Ö.: Water-soluble organic
593 carbon aerosols during a full New Delhi winter: Isotope-based source apportionment and optical properties, *J.*
594 *Geophys. Res.-Atmos.*, 119, 3476-3485, 10.1002/2013jd020041, 2014b.

595 Kirillova, E. N., Marinoni, A., Bonasoni, P., Vuillermoz, E., Facchini, M. C., Fuzzi, S., and Decesari, S.: Light
596 absorption properties of brown carbon in the high Himalayas, *J. Geophys. Res.-Atmos.*, 121, 9621-9639,
597 10.1002/2016jd025030, 2016.

598 Kitanovski, Z., Grgić, I., Vermeylen, R., Claeys, M., and Maenhaut, W.: Liquid chromatography tandem mass
599 spectrometry method for characterization of monoaromatic nitro-compounds in atmospheric particulate matter,
600 *Journal of Chromatography A*, 1268, 35-43, <https://doi.org/10.1016/j.chroma.2012.10.021>, 2012.

601 Kitanovski, Z., Čusak, A., Grgić, I., and Claeys, M.: Chemical characterization of the main products formed through
602 aqueous-phase photolysis of guaiacol, *Atmos. Meas. Tech.*, 7, 2457-2470, 10.5194/amt-7-2457-2014, 2014.

603 Kondo, Y., Miyazaki, Y., Takegawa, N., Miyakawa, T., Weber, R. J., Jimenez, J. L., Zhang, Q., and Worsnop, D. R.:
604 Oxygenated and water-soluble organic aerosols in Tokyo, *Journal of Geophysical Research*, 112, doi:
605 10.1029/2006jd007056, 10.1029/2006jd007056, 2007.

606 Laskin, A., Laskin, J., and Nizkorodov, S. A.: Chemistry of Atmospheric Brown Carbon, *Chemical reviews*, 4335-
607 4382, 10.1021/cr5006167, 2015.

608 Laskin, J., Laskin, A., Roach, P. J., Slysz, G. W., Anderson, G. A., Nizkorodov, S. A., Bones, D. L., and Nguyen, L.
609 Q.: High-Resolution Desorption Electrospray Ionization Mass Spectrometry for Chemical Characterization of
610 Organic Aerosols, *Analytical Chemistry*, 82, 2048-2058, 10.1021/ac902801f, 2010.

611 Lee, H. J., Aiona, P. K., Laskin, A., Laskin, J., and Nizkorodov, S. A.: Effect of Solar Radiation on the Optical
612 Properties and Molecular Composition of Laboratory Proxies of Atmospheric Brown Carbon, *Environ. Sci.
613 Technol.*, 48, 10217-10226, 10.1021/es502515r, 2014.

614 Li, J., Wang, G., Aggarwal, S. G., Huang, Y., Ren, Y., Zhou, B., Singh, K., Gupta, P. K., Cao, J., and Zhang, R.:
615 Comparison of abundances, compositions and sources of elements, inorganic ions and organic compounds in
616 atmospheric aerosols from Xi'an and New Delhi, two megacities in China and India, *Science of The Total
617 Environment*, 476-477, 485-495, <http://dx.doi.org/10.1016/j.scitotenv.2014.01.011>, 2014.

618 Li, J. J.: Chemical Composition, Size distribution and Source Apportionment of Atmospheric Aerosols at an Alpine
619 Site in Guanzhong Plain, China (in Chinese), Ph. D, Xi'an Jiaotong University, Xi'an, 124 pp., 2011.

620 Li, X., Chen, Y., and Bond, T. C.: Light absorption of organic aerosol from pyrolysis of corn stalk, *Atmos. Environ.*,
621 144, 249-256, <https://doi.org/10.1016/j.atmosenv.2016.09.006>, 2016a.

622 Li, X., Jiang, L., Hoa, L. P., Lyu, Y., Xu, T. T., Yang, X., Iinuma, Y., Chen, J. M., and Herrmann, H.: Size distribution
623 of particle-phase sugar and nitrophenol tracers during severe urban haze episodes in Shanghai, *Atmos.
624 Environ.*, 145, 115-127, 10.1016/j.atmosenv.2016.09.030, 2016b.

625 Lin, P., Liu, J., Shilling, J. E., Kathmann, S. M., Laskin, J., and Laskin, A.: Molecular characterization of brown
626 carbon (BrC) chromophores in secondary organic aerosol generated from photo-oxidation of toluene, *Phys
627 Chem Chem Phys*, 17, 23312-23325, 10.1039/c5cp02563j, 2015.

628 Lin, P., Bluvshstein, N., Rudich, Y., Nizkorodov, S. A., Laskin, J., and Laskin, A.: Molecular Chemistry of
629 Atmospheric Brown Carbon Inferred from a Nationwide Biomass Burning Event, *Environ Sci Technol*, 51,
630 11561-11570, 10.1021/acs.est.7b02276, 2017.

631 Lin, Y.-H., Budisulistiorini, S. H., Chu, K., Siejack, R. A., Zhang, H., Riva, M., Zhang, Z., Gold, A., Kautzman, K.
632 E., and Surratt, J. D.: Light-Absorbing Oligomer Formation in Secondary Organic Aerosol from Reactive
633 Uptake of Isoprene Epoxydiols, *Environ. Sci. Technol.*, 48, 12012-12021, 10.1021/es503142b, 2014.

634 Liu, J., Bergin, M., Guo, H., King, L., Kotra, N., Edgerton, E., and Weber, R. J.: Size-resolved measurements of
635 brown carbon in water and methanol extracts and estimates of their contribution to ambient fine-particle light
636 absorption, *Atmos. Chem. Phys.*, 13, 12389-12404, 10.5194/acp-13-12389-2013, 2013.

637 Liu, J., Lin, P., Laskin, A., Laskin, J., Kathmann, S. M., Wise, M., Caylor, R., Imholt, F., Selimovic, V., and Shilling,
638 J. E.: Optical properties and aging of light-absorbing secondary organic aerosol, *Atmos. Chem. Phys.*, 16,
639 12815-12827, 10.5194/acp-16-12815-2016, 2016.

640 Liu, J., Mo, Y., Ding, P., Li, J., Shen, C., and Zhang, G.: Dual carbon isotopes (C-14 and C-13) and optical
641 properties of WSOC and HULIS-C during winter in Guangzhou, China, *Science of the Total Environment*, 633,
642 1571-1578, 10.1016/j.scitotenv.2018.03.293, 2018.

643 Liu, P. F., Abdelmalki, N., Hung, H. M., Wang, Y., Brune, W. H., and Martin, S. T.: Ultraviolet and visible complex
644 refractive indices of secondary organic material produced by photooxidation of the aromatic compounds
645 toluene and m-xylene, *Atmos. Chem. Phys.*, 15, 1435-1446, 10.5194/acp-15-1435-2015, 2015.

646 Lu, J. W., Flores, J. M., Lavi, A., Abo-Riziq, A., and Rudich, Y.: Changes in the optical properties of
647 benzo[a]pyrene-coated aerosols upon heterogeneous reactions with NO₂ and NO₃, *Physical Chemistry
648 Chemical Physics*, 13, 6484-6492, 10.1039/C0CP02114H, 2011.

649 Mohr, C., Lopez-Hilfiker, F. D., Zotter, P., Prévôt, A. S. H., Xu, L., Ng, N. L., Herndon, S. C., Williams, L. R.,

650 Franklin, J. P., Zahniser, M. S., Worsnop, D. R., Knighton, W. B., Aiken, A. C., Gorkowski, K. J., Dubey, M.
651 K., Allan, J. D., and Thornton, J. A.: Contribution of Nitrated Phenols to Wood Burning Brown Carbon Light
652 Absorption in Detling, United Kingdom during Winter Time, *Environ. Sci. Technol.*, 47, 6316-6324,
653 10.1021/es400683v, 2013.

654 Moschos, V., Kumar, N. K., Daellenbach, K. R., Baltensperger, U., Prévôt, A. S. H., and El Haddad, I.: Source
655 Apportionment of Brown Carbon Absorption by Coupling Ultraviolet–Visible Spectroscopy with Aerosol Mass
656 Spectrometry, *Environmental Science & Technology Letters*, 5, 302-308, 10.1021/acs.estlett.8b00118, 2018.

657 Nakayama, T., Sato, K., Matsumi, Y., Imamura, T., Yamazaki, A., and Uchiyama, A.: Wavelength Dependence of
658 Refractive Index of Secondary Organic Aerosols Generated during the Ozonolysis and Photooxidation of
659 α -Pinene, *SOLA*, 8, 119-123, 10.2151/sola.2012-030, 2012.

660 Nakayama, T., Sato, K., Tsuge, M., Imamura, T., and Matsumi, Y.: Complex refractive index of secondary organic
661 aerosol generated from isoprene/NO_x photooxidation in the presence and absence of SO₂, *J. Geophys. Res.-*
662 *Atmos.*, 120, 7777-7787, 10.1002/2015jd023522, 2015.

663 Nguyen, T. B., Lee, P. B., Updyke, K. M., Bones, D. L., Laskin, J., Laskin, A., and Nizkorodov, S. A.: Formation of
664 nitrogen- and sulfur-containing light-absorbing compounds accelerated by evaporation of water from secondary
665 organic aerosols, *J. Geophys. Res.-Atmos.*, 117, 14, 10.1029/2011jd016944, 2012.

666 Nozière, B., and Esteve, W.: Organic reactions increasing the absorption index of atmospheric sulfuric acid aerosols,
667 *Geophysical Research Letters*, 32, doi:10.1029/2004GL021942, 10.1029/2004gl021942, 2005.

668 Nozière, B., Dziedzic, P., and Córdoba, A.: Formation of secondary light-absorbing “fulvic-like” oligomers: A
669 common process in aqueous and ionic atmospheric particles?, *Geophysical Research Letters*, 34,
670 doi:10.1029/2007GL031300, 10.1029/2007gl031300, 2007.

671 Ofner, J., Krüger, H. U., Grothe, H., Schmitt-Kopplin, P., Whitmore, K., and Zetzsch, C.: Physico-chemical
672 characterization of SOA derived from catechol and guaiacol – a model substance for the aromatic
673 fraction of atmospheric HULIS, *Atmos. Chem. Phys.*, 11, 1-15, 10.5194/acp-11-1-2011, 2011.

674 Park, S. S., and Yu, J.: Chemical and light absorption properties of humic-like substances from biomass burning
675 emissions under controlled combustion experiments, *Atmos. Environ.*, 136, 114-122,
676 <https://doi.org/10.1016/j.atmosenv.2016.04.022>, 2016.

677 Powelson, M. H., Espelien, B. M., Hawkins, L. N., Galloway, M. M., and De Haan, D. O.: Brown Carbon Formation
678 by Aqueous-Phase Carbonyl Compound Reactions with Amines and Ammonium Sulfate, *Environ. Sci.*
679 *Technol.*, 48, 985-993, 10.1021/es4038325, 2014.

680 Rizzo, L. V., Correia, A. L., Artaxo, P., Procópio, A. S., and Andreae, M. O.: Spectral dependence of aerosol light
681 absorption over the Amazon Basin, *Atmos. Chem. Phys.*, 11, 8899-8912, 10.5194/acp-11-8899-2011, 2011.

682 Rizzo, L. V., Artaxo, P., Müller, T., Wiedensohler, A., Paixão, M., Cirino, G. G., Arana, A., Swietlicki, E., Roldin, P.,
683 Fors, E. O., Wiedemann, K. T., Leal, L. S. M., and Kulmala, M.: Long term measurements of aerosol optical
684 properties at a primary forest site in Amazonia, *Atmos. Chem. Phys.*, 13, 2391-2413, 10.5194/acp-13-2391-
685 2013, 2013.

686 Romonosky, D. E., Laskin, A., Laskin, J., and Nizkorodov, S. A.: High-Resolution Mass Spectrometry and
687 Molecular Characterization of Aqueous Photochemistry Products of Common Types of Secondary Organic
688 Aerosols, *The Journal of Physical Chemistry A*, 119, 2594-2606, 10.1021/jp509476r, 2015.

689 Samburova, V., Connolly, J., Gyawali, M., Yatavelli, R. L. N., Watts, A. C., Chakrabarty, R. K., Zielinska, B.,
690 Moosmüller, H., and Khlystov, A.: Polycyclic aromatic hydrocarbons in biomass-burning emissions and their
691 contribution to light absorption and aerosol toxicity, *Science of The Total Environment*, 568, 391-401,
692 <https://doi.org/10.1016/j.scitotenv.2016.06.026>, 2016.

693 Sengupta, D., Samburova, V., Bhattarai, C., Kirillova, E., Mazzoleni, L., Iaukea-Lum, M., Watts, A., Moosmüller,

694 H., and Khlystov, A.: Light absorption by polar and non-polar aerosol compounds from laboratory biomass
695 combustion, *Atmos. Chem. Phys.*, 18, 10849-10867, 10.5194/acp-18-10849-2018, 2018.

696 Shen, Z., Zhang, Q., Cao, J., Zhang, L., Lei, Y., Huang, Y., Huang, R. J., Gao, J., Zhao, Z., Zhu, C., Yin, X., Zheng,
697 C., Xu, H., and Liu, S.: Optical properties and possible sources of brown carbon in PM 2.5 over Xi'an, China,
698 *Atmos. Environ.*, 150, 322-330, 10.1016/j.atmosenv.2016.11.024, 2017.

699 Simoneit, B. R. T.: Biomass burning - A review of organic tracers for smoke from incomplete combustion, *Applied*
700 *Geochemistry*, 17, 129-162, 2002.

701 Smith, J. D., Kinney, H., and Anastasio, C.: Phenolic carbonyls undergo rapid aqueous photodegradation to form
702 low-volatility, light-absorbing products, *Atmos. Environ.*, 126, 36-44, 10.1016/j.atmosenv.2015.11.035, 2016.

703 Sumlin, B. J., Pandey, A., Walker, M. J., Pattison, R. S., Williams, B. J., and Chakrabarty, R. K.: Atmospheric
704 Photooxidation Diminishes Light Absorption by Primary Brown Carbon Aerosol from Biomass Burning,
705 *Environmental Science & Technology Letters*, 4, 540-545, 10.1021/acs.estlett.7b00393, 2017.

706 Sun, H., Biedermann, L., and Bond, T. C.: Color of brown carbon: A model for ultraviolet and visible light
707 absorption by organic carbon aerosol, *Geophysical Research Letters*, 34, doi: 10.1029/2007gl029797,
708 10.1029/2007gl029797, 2007.

709 Teich, M., van Pinxteren, D., Wang, M., Kecorius, S., Wang, Z., Müller, T., Močnik, G., and Herrmann, H.:
710 Contributions of nitrated aromatic compounds to the light absorption of water-soluble and particulate brown
711 carbon in different atmospheric environments in Germany and China, *Atmos. Chem. Phys.*, 17, 1653-1672,
712 10.5194/acp-17-1653-2017, 2017.

713 Tran, A., Williams, G., Younus, S., Ali, N. N., Blair, S. L., Nizkorodov, S. A., and Al-Abadleh, H. A.: Efficient
714 Formation of Light-Absorbing Polymeric Nanoparticles from the Reaction of Soluble Fe(III) with C4 and C6
715 Dicarboxylic Acids, *Environ. Sci. Technol.*, 51, 9700-9708, 10.1021/acs.est.7b01826, 2017.

716 Updyke, K. M., Nguyen, T. B., and Nizkorodov, S. A.: Formation of brown carbon via reactions of ammonia with
717 secondary organic aerosols from biogenic and anthropogenic precursors, *Atmos. Environ.*, 63, 22-31,
718 <https://doi.org/10.1016/j.atmosenv.2012.09.012>, 2012.

719 van Donkelaar, A., Martin, R. V., Brauer, M., Kahn, R., Levy, R., Verduzco, C., and Villeneuve, P. J.: Global
720 Estimates of Ambient Fine Particulate Matter Concentrations from Satellite-Based Aerosol Optical Depth:
721 Development and Application, *Environmental Health Perspectives*, 118, 847-855, 10.1289/ehp.0901623, 2010.

722 Wang, G. H., Zhang, R. Y., Gomez, M. E., Yang, L. X., Zamora, M. L., Hu, M., Lin, Y., Peng, J. F., Guo, S., Meng,
723 J. J., Li, J. J., Cheng, C. L., Hu, T. F., Ren, Y. Q., Wang, Y. S., Gao, J., Cao, J. J., An, Z. S., Zhou, W. J., Li, G.
724 H., Wang, J. Y., Tian, P. F., Marrero-Ortiz, W., Secret, J., Du, Z. F., Zheng, J., Shang, D. J., Zeng, L. M., Shao,
725 M., Wang, W. G., Huang, Y., Wang, Y., Zhu, Y. J., Li, Y. X., Hu, J. X., Pan, B., Cai, L., Cheng, Y. T., Ji, Y. M.,
726 Zhang, F., Rosenfeld, D., Liss, P. S., Duce, R. A., Kolb, C. E., and Molina, M. J.: Persistent sulfate formation
727 from London Fog to Chinese haze, *Proceedings of the National Academy of Sciences of the United States of*
728 *America*, 113, 13630-13635, 10.1073/pnas.1616540113, 2016.

729 Washenfelder, R. A., Attwood, A. R., Brock, C. A., Guo, H., Xu, L., Weber, R. J., Ng, N. L., Allen, H. M., Ayres, B.
730 R., Baumann, K., Cohen, R. C., Draper, D. C., Duffey, K. C., Edgerton, E., Fry, J. L., Hu, W. W., Jimenez, J. L.,
731 Palm, B. B., Romer, P., Stone, E. A., Wooldridge, P. J., and Brown, S. S.: Biomass burning dominates brown
732 carbon absorption in the rural southeastern United States, *Geophysical Research Letters*, 42, 653-664,
733 doi:10.1002/2014GL062444, 2015.

734 Wu, C.: Seasonal variation of atmospheric acidic and basic species and the characteristics of gas-particle partition in
735 a typical city of Guanzhong Basin (in Chinese), Ph. D, The University of Chinese Academy of Sciences, The
736 University of Chinese Academy of Sciences, Xi'an, 2018.

737 Wu, C., Wang, G., Wang, J., Li, J., Ren, Y., Zhang, L., Cao, C., Li, J., Ge, S., Xie, Y., Wang, X., and Xue, G.:

738 Chemical characteristics of haze particles in Xi'an during Chinese Spring Festival: Impact of fireworks burning,
739 Journal of Environmental Sciences, 71, 179-187, <https://doi.org/10.1016/j.jes.2018.04.008>, 2018.

740 Wu, C., Wang, G., Li, J., Li, J., Cao, C., Ge, S., Xie, Y., Chen, J., Li, X., Xue, G., Wang, X., Zhao, Z., and Cao, F.:
741 The characteristics of atmospheric brown carbon in Xi'an, inland China: sources, size distributions and optical
742 properties, Atmos. Chem. Phys., 20, 2017-2030, 10.5194/acp-20-2017-2020, 2020.

743 Wu, G., Ram, K., Fu, P., Wang, W., Zhang, Y., Liu, X., Stone, E. A., Pradhan, B. B., Dangol, P. M., Panday, A. K.,
744 Wan, X., Bai, Z., Kang, S., Zhang, Q., and Cong, Z.: Water-Soluble Brown Carbon in Atmospheric Aerosols
745 from Godavari (Nepal), a Regional Representative of South Asia, Environ. Sci. Technol., 53, 3471-3479,
746 10.1021/acs.est.9b00596, 2019.

747 Xie, M., Chen, X., Hays, M. D., and Holder, A. L.: Composition and light absorption of N-containing aromatic
748 compounds in organic aerosols from laboratory biomass burning, Atmos. Chem. Phys., 19, 2899-2915,
749 10.5194/acp-19-2899-2019, 2019.

750 Xu, J., Cui, T. Q., Fowler, B., Fankhauser, A., Yang, K., Surratt, J. D., and McNeill, V. F.: Aerosol Brown Carbon
751 from Dark Reactions of Syringol in Aqueous Aerosol Mimics, Acs Earth and Space Chemistry, 2, 608-617,
752 10.1021/acsearthspacechem.8b00010, 2018.

753 Xu, J., Hettiyadura, A. P. S., Liu, Y., Zhang, X., Kang, S., and Laskin, A.: Regional Differences of Chemical
754 Composition and Optical Properties of Aerosols in the Tibetan Plateau, Journal of Geophysical Research:
755 Atmospheres, 125, 10.1029/2019jd031226, 2020.

756 Yan, C., Zheng, M., Sullivan, A. P., Bosch, C., Desyaterik, Y., Andersson, A., Li, X., Guo, X., Zhou, T., Gustafsson,
757 Ö., and Collett, J. L.: Chemical characteristics and light-absorbing property of water-soluble organic carbon in
758 Beijing: Biomass burning contributions, Atmos. Environ., 121, 4-12,
759 <https://doi.org/10.1016/j.atmosenv.2015.05.005>, 2015a.

760 Yan, C., Zheng, M., Sullivan, A. P., Bosch, C., Desyaterik, Y., Andersson, A., Li, X., Guo, X., Zhou, T., Gustafsson,
761 O., and Collett, J. L., Jr.: Chemical characteristics and light-absorbing property of water-soluble organic carbon
762 in Beijing: Biomass burning contributions, Atmos. Environ., 121, 4-12, 10.1016/j.atmosenv.2015.05.005,
763 2015b.

764 Yan, C. Q., Zheng, M., Bosch, C., Andersson, A., Desyaterik, Y., Sullivan, A. P., Collett, J. L., Zhao, B., Wang, S.
765 X., He, K. B., and Gustafsson, O.: Important fossil source contribution to brown carbon in Beijing during
766 winter, Scientific reports, 7, DOI: 10.1038/srep43182, 10.1038/srep43182, 2017.

767 Yu, L., Smith, J., Laskin, A., Anastasio, C., Laskin, J., and Zhang, Q.: Chemical characterization of SOA formed
768 from aqueous-phase reactions of phenols with the triplet excited state of carbonyl and hydroxyl radical, Atmos.
769 Chem. Phys., 14, 13801-13816, 10.5194/acp-14-13801-2014, 2014.

770 Zhang, X., Lin, Y.-H., Surratt, J. D., and Weber, R. J.: Sources, Composition and Absorption Ångström Exponent of
771 Light-absorbing Organic Components in Aerosol Extracts from the Los Angeles Basin, Environ. Sci. Technol.,
772 47, 3685-3693, 10.1021/es305047b, 2013.

773 Zhao, R., Lee, A. K. Y., Huang, L., Li, X., Yang, F., and Abbatt, J. P. D.: Photochemical processing of aqueous
774 atmospheric brown carbon, Atmos. Chem. Phys., 15, 6087-6100, 10.5194/acp-15-6087-2015, 2015.

775

776 Table 1 Average ($\pm 1\sigma$) values Abs_{365} , MAC_{365} , and AAE of WS-BrC and WI-BrC, as well as concentrations of
 777 OC, WSOC, WIOC, and measured organic species in the $\text{PM}_{2.5}$ aerosols from the rural site of Guanzhong Basin.

	Summer			Winter		
	Average	Daytime	Nighttime	Average	Daytime	Nighttime
$\text{Abs}_{365, \text{WS-BrC}}$ (Mm^{-1})	5.00 \pm 1.28	5.64 \pm 1.34	4.37 \pm 0.83	19.6 \pm 8.3	19.2 \pm 6.8	19.9 \pm 9.5
$\text{Abs}_{365, \text{WI-BrC}}$ (Mm^{-1})	2.95 \pm 1.94	4.23 \pm 1.93	1.67 \pm 0.72	21.9 \pm 13.5	17.2 \pm 8.2	26.7 \pm 15.8
$\text{MAC}_{365, \text{WS-BrC}}$ ($\text{m}^2 \text{g}^{-1}$)	1.00 \pm 0.18	0.99 \pm 0.17	1.01 \pm 0.18	0.93 \pm 0.25	0.92 \pm 0.21	0.94 \pm 0.28
$\text{MAC}_{365, \text{WI-BrC}}$ ($\text{m}^2 \text{g}^{-1}$)	1.82 \pm 1.06	2.45 \pm 1.14	1.18 \pm 0.36	0.95 \pm 0.32	0.85 \pm 0.34	1.05 \pm 0.28
$\text{AAE}_{\text{WS-BrC}}$	5.43 \pm 0.41	5.56 \pm 0.4	5.30 \pm 0.38	5.11 \pm 0.53	5.14 \pm 0.2	5.07 \pm 0.72
$\text{AAE}_{\text{WI-BrC}}$	5.01 \pm 0.58	4.74 \pm 0.19	5.28 \pm 0.71	6.04 \pm 0.22	5.94 \pm 0.12	6.15 \pm 0.24
OC ($\mu\text{g m}^{-3}$)	6.78 \pm 1.77	7.74 \pm 1.73	5.83 \pm 1.19	45.9 \pm 22.9	44.0 \pm 17.2	47.9 \pm 27.2
WSOC ($\mu\text{g m}^{-3}$)	5.06 \pm 1.11	5.72 \pm 1.02	4.39 \pm 0.72	21.9 \pm 9.3	22.1 \pm 8.0	21.7 \pm 10.4
WIOC ($\mu\text{g m}^{-3}$)	1.73 \pm 0.87	2.02 \pm 1.04	1.44 \pm 0.53	24.0 \pm 14.3	21.9 \pm 10.1	26.2 \pm 17.3
WSOC/OC	0.75 \pm 0.07	0.75 \pm 0.09	0.76 \pm 0.04	0.50 \pm 0.09	0.51 \pm 0.08	0.48 \pm 0.10
Parent-PAHs (ng m^{-3})	8.81 \pm 5.09	11.6 \pm 5.7	5.98 \pm 1.9	82.3 \pm 53.7	70.8 \pm 35.4	93.9 \pm 65.1
OPAHs (ng m^{-3})	14.0 \pm 14.0	23.0 \pm 15.1	4.97 \pm 1.34	98.3 \pm 59.5	89.4 \pm 39.8	107 \pm 73
Nitrophenols (ng m^{-3})	0.94 \pm 0.26	0.87 \pm 0.26	1.02 \pm 0.24	72.6 \pm 63.7	41.1 \pm 15.5	104 \pm 77
SOA_i^a (ng m^{-3})	18.6 \pm 9.7	15.0 \pm 8.0	22.1 \pm 9.8	BDL ^c	BDL	BDL
SOA_p^b (ng m^{-3})	22.0 \pm 6.7	25.2 \pm 6.7	18.9 \pm 5.0	BDL	BDL	BDL
Levogluconan (ng m^{-3})	98.7 \pm 83.7	142 \pm 89	55.1 \pm 48.7	601 \pm 301	569 \pm 138	633 \pm 401

778 ^a SOA_i : Tracers of SOA formed from isoprene (SOA_i) oxidation, i.e., the sum of 2-methylglyceric acid, 2-methylthreitol, and 2-
 779 methylerythritol.

780 ^b SOA_p : Tracers of SOA formed from α -/ β -pinene (SOA_p) oxidation, i.e., the sum of pinonic acid, pinic acid, and 3-methyl-1,2,3-
 781 butanetricarboxylic acid.

782 ^c BDL: below detection limit ($<0.17 \text{ ng m}^{-3}$).

783

784

785

786 Table 2 Comparison of MAC_{365,WS-BrC} in the present study and those reported in earlier studies in China, India, and
 787 the United States (US).

Sampling site	Sampling time	Season	MAC _{365,WS-BrC} (m ² g ⁻¹)	Reference
Lincun, Shaanxi, China	Aug. 3-23, 2016	Summer	1.00±0.18	This study
	Jan. 20-Feb 1, 2017	Winter	0.93±0.25	
Xi'an, China	Jun. 1-Aug. 31, 2009	Summer	0.98 ±0.21	Huang et al. (2018)
	Nov.15, 2008-Mar. 14, 2009	Winter	1.65 ± 0.36	
Beijing, China	Jun. 20-Jul. 20, 2009	Summer	1.8 ± 0.2	Cheng et al. (2011)
	Jan.9-Feb. 12, 2009	Winter	0.7 ± 0.2	
<u>XiangHe, Hebei, China</u>	<u>Jul. 9-14 and Jul. 21-Aug. 1, 2013</u>	<u>Summer</u>	<u>0.38 ± 0.52^a</u>	Teich et al. (2017)
<u>Wangdu, Hebei, China</u>	<u>Jun. 4-24, 2014</u>	<u>Summer</u>	<u>0.55 ± 0.15^a</u>	
<u>Mt. Waliguan, Qinghai, China</u>	<u>Jul. 1-31, 2017</u>	<u>Summer</u>	<u>0.48</u>	Xu et al. (2020)
Seoul, Korea	Aug. 13-Sep. 9, 2013	Summer	0.28	Kim et al. (2016)
	Jan. 9-Feb 8, 2013	Winter	1.02	
New Delhi, India	Oct. 24, 2010-Mar. 25, 2011	Winter	1.6 ± 0.5	Kirillova et al. (2014b)
Los Angeles Basin, US	mid-May - mid-June, 2010	summer Summer	0.71	Zhang et al. (2013)
Southeastern US	2007	annually Annually	0.3-0.7	Hecobian et al. (2010)
Atlanta, US	May 17-Sep. 29, 2012	summer Summer and fall Fall	0.14-0.53	Liu et al. (2013)

788 ^aData at XiangHe and Wangdu were the averaged MAC of WSOC at wavelength of 370 nm (i.e., MAC_{370,WS-BrC})

789

790

791

792 Table 3 Average direct solar absorption of water-soluble and water-insoluble BrC during summer and winter

	WSOC		WIOC	
	Summer	Winter	Summer	Winter
<i>Actinic flux (×10¹⁴ quanta s⁻¹ cm⁻²)</i>				
300-400 nm	1.55±0.43	2.14±0.92	1.03±0.64	2.53±1.52
400-700 nm	1.77±0.6	2.67±1.04	1.24±0.8	2.58±1.48
<i>Irradiance (W m⁻²)</i>				
300-400 nm	0.51±0.14	0.57±0.25	0.34±0.21	0.68±0.41
400-700 nm	0.49±0.17	0.57±0.22	0.35±0.23	0.55±0.32
<i>Relative to EC (%)</i>				
300-400 nm	49.4±14.5	25.9±5.47	29.4±11.0	29.0±10.4
400-700 nm	10.0±3.52	4.99±1.23	6.19±2.42	4.51±1.44

793

794

Figure Caption

795

796 Figure 1 Temporal variation of meteorological parameters (a and b), concentrations of major
797 chemical compositions, Abs_{365} , MAC_{365} , and AAE of water-soluble and water-insoluble
798 BrC in $PM_{2.5}$ from the rural area of Northwest China.

799

800 Figure 2 Average spectra of absorption coefficient (Abs_{λ}) (a,b) and mass absorption coefficient
801 (MAC_{λ}) (c,d) of water-soluble (WS-BrC) and water-insoluble (WI-BrC) BrC, ~~as well as the~~
802 ~~ratio of $MAC_{\lambda, WI-BrC}$ to $MAC_{\lambda, WS-BrC}$ (e,f)~~ during daytime and nighttime of summer and
803 winter. Absorption Ångström exponent (AAE) is calculated by a linear regression of log
804 Abs_{λ} versus log λ in the wavelength range of 300–450 nm.

805

806 Figure 3 Cross correlations between $Abs_{365, WS-BrC}$, $Abs_{365, WI-BrC}$, selected chemical compositions,
807 and RH in summer. The numbers at the upper right denote the linear correlation coefficients
808 (r^2) of the corresponding scatter plots.

809

810 Figure 4 Cross correlations between $Abs_{365, WS-BrC}$, $Abs_{365, WI-BrC}$, selected chemical compositions,
811 and RH in winter. The numbers at the upper right denote the linear correlation coefficients
812 (r^2) of the corresponding scatter plots.

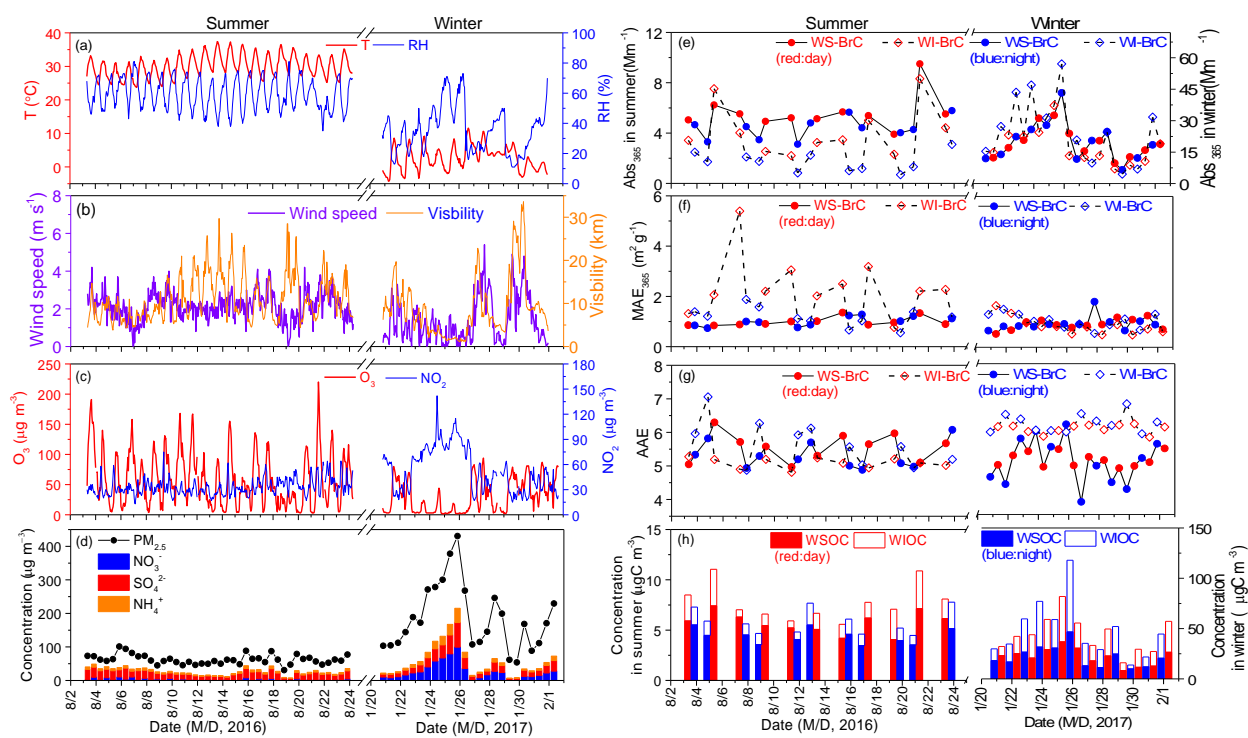
813

814 Figure 5 Average contribution of parent-PAHs and OPAHs to the bulk light absorption of WI-
815 BrC (300–700 nm) during daytime and nighttime of summer and winter.

816

817

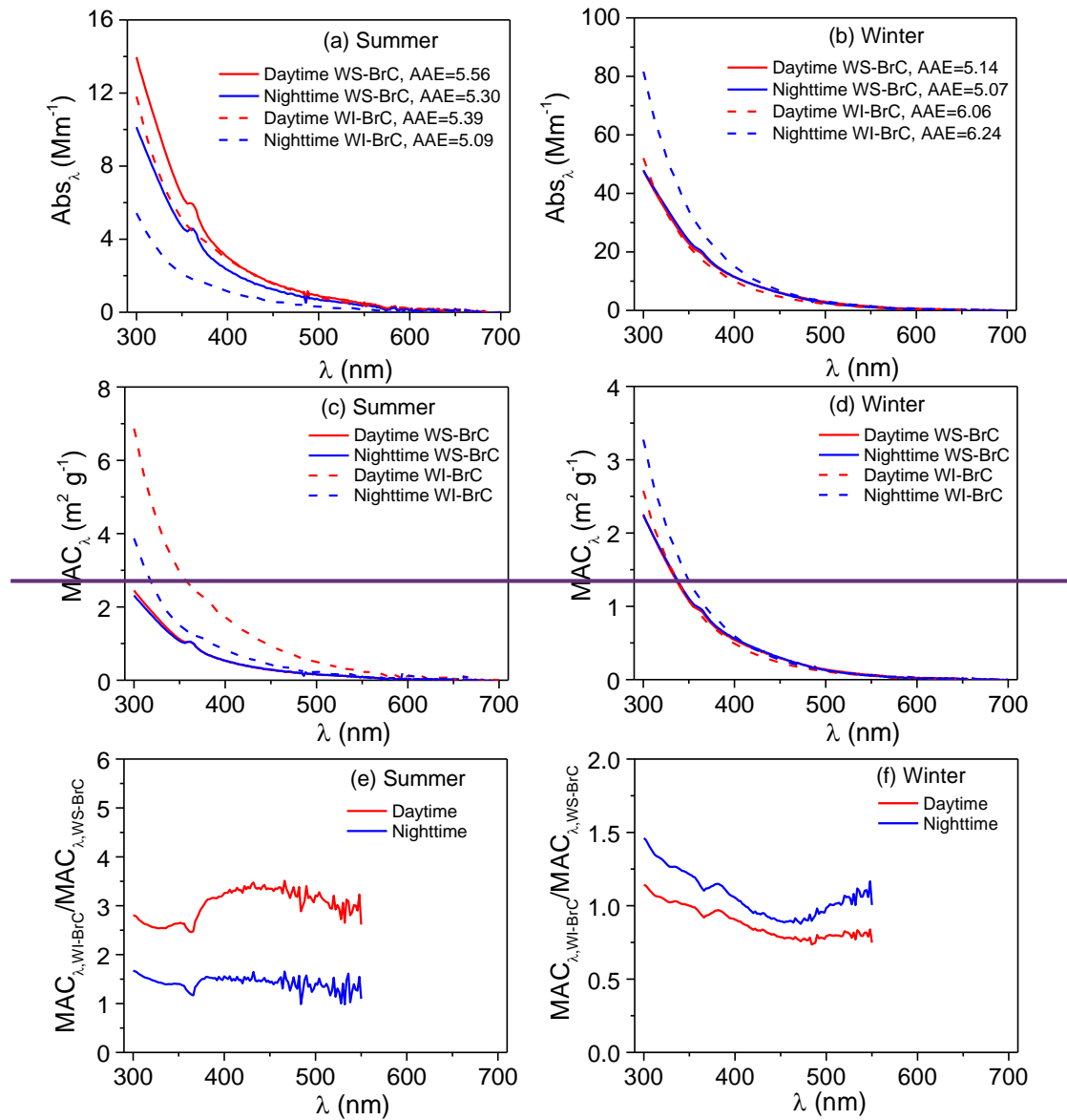
818

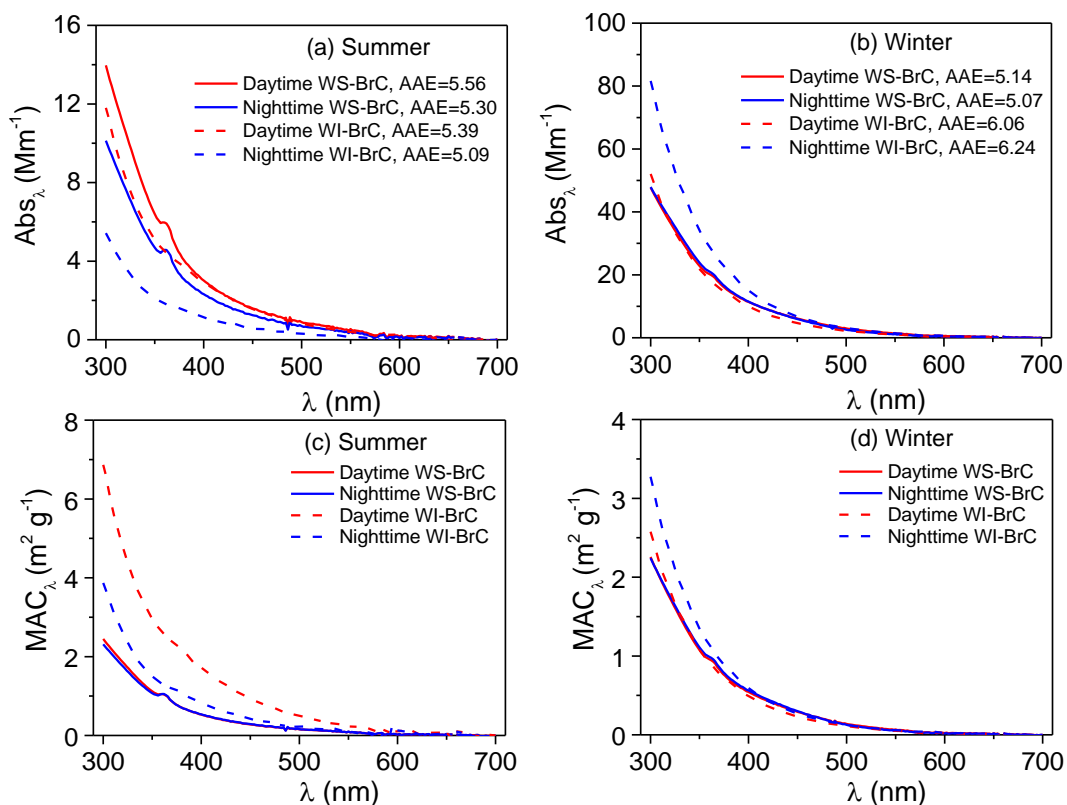


820

821 Figure 1 Temporal variation of meteorological parameters (a and b), concentrations of major chemical
 822 compositions, Abs₃₆₅, MAC₃₆₅, and AAE of water-soluble and water-insoluble BrC in PM_{2.5} from the rural
 823 area of Northwest China.

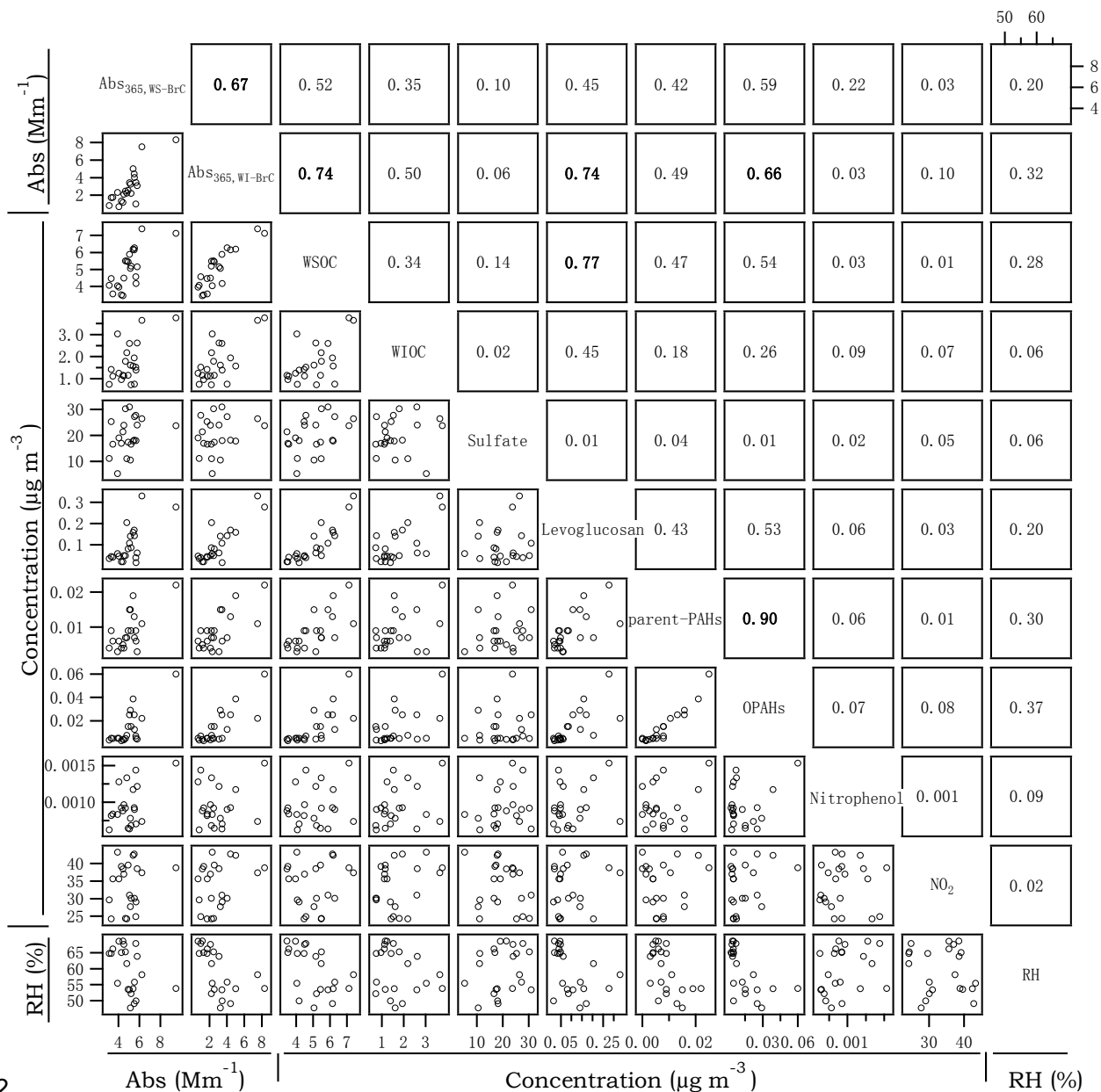
824





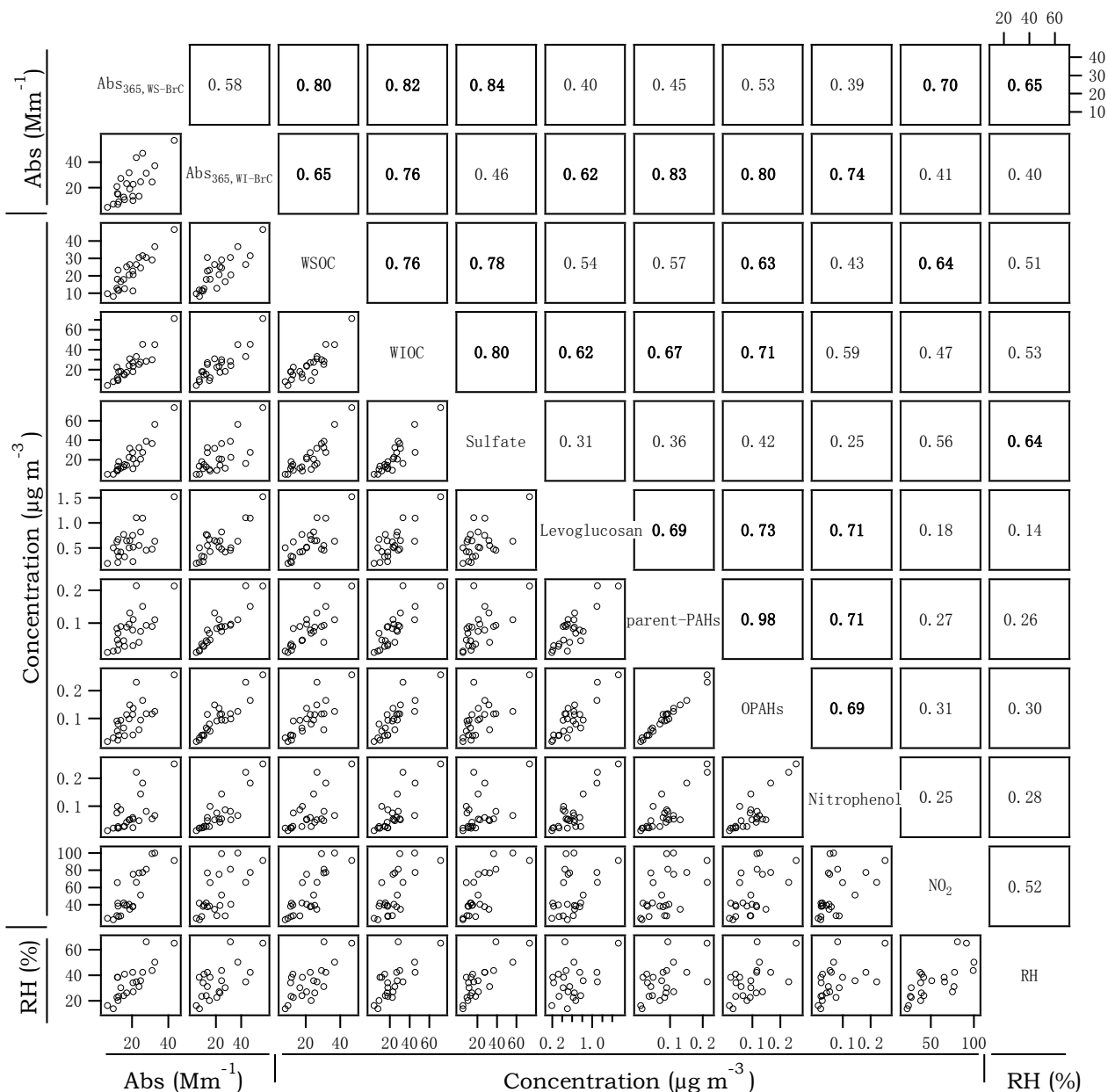
826

827 Figure 2 Average spectra of absorption coefficient (Abs_{λ}) (a,b) and mass absorption coefficient (MAC_{λ}) (c,d)
 828 of water-soluble (WS-BrC) and water-insoluble (WI-BrC) BrC, as well as the ratio of $MAC_{\lambda,WI-BrC}$ to $MAC_{\lambda,WS-BrC}$
 829 (e,f) during daytime and nighttime of summer and winter. Absorption Ångström exponent (AAE) is
 830 calculated by a linear regression of $\log Abs_{\lambda}$ versus $\log \lambda$ in the wavelength range of 300–450 nm.
 831



832
833
834
835
836

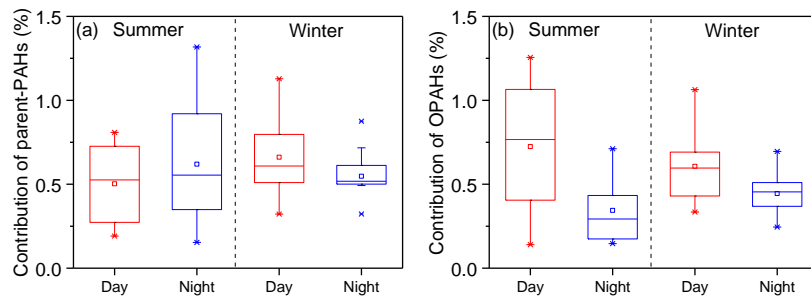
Figure 3 Cross-correlations between Abs_{365,WS-BrC}, Abs_{365,WI-BrC}, selected chemical components, and RH in summer. The numbers at the upper right denote the linear correlation coefficients (r^2) of the corresponding scatter plots.



837

838 Figure 4 Cross-correlations between Abs_{365,WS-BrC}, Abs_{365,WI-BrC}, selected chemical components, and RH in
 839 winter. The numbers at the upper right denote the linear correlation coefficients (r^2) of the corresponding
 840 scatter plots.

841



842

843 Figure 5 Average contribution of parent-PAHs and OPAHs to the bulk light absorption of WI-BrC (300–700
 844 nm) during daytime and nighttime of summer and winter.

845

846

Supporting information

Optical properties, molecular compositions and secondary formation of Brown carbon (BrC) in a rural area of Guanzhong Basin, China

Jianjun Li^{1,2}, Qi Zhang^{2,*}, Gehui Wang^{1,3,4,*}, Jin Li¹, Can Wu^{1,3}, Lang Liu¹, Jiayuan

Wang^{1,2}, Wenqing Jiang², Lijuan Li^{1,2}, Kin Fai Ho^{1,5}, Junji Cao¹

¹ Key Lab of Aerosol Chemistry & Physics, SKLLQG, Institute of Earth Environment, Chinese Academy of Sciences, Xi'an 710061, China

² Department of Environmental Toxicology, University of California, Davis, CA 95616, USA

³ Key Laboratory of Geographic Information Science of the Ministry of Education, School of Geographic Sciences, East China Normal University, Shanghai 200241, China

⁴ Institute of Eco-Chongming, 3663 N. Zhongshan Rd., Shanghai 200062, China

⁵ The Jockey Club School of Public Health and Primary Care, The Chinese University of Hong Kong, Hong Kong, China

*Corresponding authors:

Prof. Qi Zhang

Department of Environmental Toxicology, University of California, Davis
One Shields Avenue, Davis, CA 95616

Phone: 1-530-752-5779

Fax: 1-530-752-3394

Email: dkwzhang@ucdavis.edu;

Prof. Gehui Wang

School of Geographic Sciences, East China Normal University, Shanghai, China
500 Dongchuan Rd., Shanghai 200241, China

Phone: 86-21-5434-1193

E-mail: ghwang@geo.ecnu.edu.cn.

Estimation of contribution of parent-PAHs and OPAHs to the light absorption of water-insoluble BrC

Average mass absorption coefficient of individual PAH (parent-PAH or OPAH) ($MAC_{PAH,AV}$) in the wavelength range of 300-700 nm in this study is cited from Samburova et al. (Samburova et al., 2016) and Huang et al. (Huang et al., 2018), who use authentic standard to measure the absorption of each individual PAH, and then calculated the $MAC_{PAH,AV}$ by multiplying MAC_{λ} of individual PAHs with the power distribution of the solar spectrum and spectrally integrated (eq S1).

$$MAC_{PAH,AV} = \frac{\int_{300}^{700} MAC_{\lambda} \times I_0(\lambda) d\lambda}{\int_{300}^{700} I_0(\lambda) d\lambda} \quad (eq S1)$$

where $I_0(\lambda)$ is the clear sky Air Mass 1 Global Horizontal solar irradiance (Levinson et al., 2010). Then the $MAC_{PAH,AV}$ were used to calculate the contribution of individual PAH to solar-spectrum-weighted absorption coefficient of WI-BrC.

Estimation of light absorption of elemental carbon

The light absorption of elemental carbon (EC) were estimated by the output data of thermal/optical carbon analyzer, which is similar to the determination of black carbon (BC) light absorption by Aethalometer (Ram and Sarin, 2009). At first, the optical-attenuation (ATN) at wavelength of 632 nm (wavelength used in carbon analyzer) caused by EC is governed by the Beer-Lambert's law, according to the eq S2.

$$ATN_{632,EC} = -\ln\left(\frac{I}{I_0}\right) \quad (eq S2)$$

where I_0 and I is the intensity of incident light and transmitted light through the filter substrate and aerosols.

Then $b_{ap,632,EC}$ can be obtained after correcting the multiple scattering and shadowing effects following by eq S4:

$$b_{ap,632,EC} = \frac{ATN_{632,EC}}{C \times R(ATN)} \times \frac{A}{V} \quad (eq S3)$$

where A is the effective filter area (414 cm^2), V is the volume of air sampled (m^3). C depends on absorbing material, mixing state of aerosols, and filter substrate, and a value of 2.14 was suggested for quartz filters (Weingartner et al., 2003; Bond and Bergstrom, 2006). $R(ATN)$ is determined by eq S4:

$$R(ATN) = \left(\frac{1}{f} - 1\right) \times \frac{\ln ATN_{632,EC} - \ln 10\%}{\ln 50\% - \ln 10\%} + 1 \quad (eq S4)$$

where f is set as 1.103 for wintertime and 1.114 for summertime (Sandradewi et al., 2008).

At last, light absorption coefficient of EC at wavelength of λ ($b_{ap,\lambda,EC}$) can be calculated by eq S5:

$$b_{ap,\lambda,EC} = b_{ap,632,EC} \times \left(\frac{632}{\lambda}\right)^{AAE} \quad (eq S5)$$

where AAE is the absorption Ångström exponent of EC. Previous study suggested that AAE of EC is in the range of 0.8 and 1.4 (Lack et al., 2013), and a value of 1.0

were used in this study.

Then the contribution of BrC relative to EC ($f_{BrC/EC}$, %) can be calculated by eq S6:

$$f_{BrC/EC} = \frac{\int I_0(\lambda)(1-e^{-b_{ap,\lambda,BrC} \times h_{ABL}})d\lambda}{\int I_0(\lambda)(1-e^{-b_{ap,\lambda,EC} \times h_{ABL}})d\lambda} \times 100 \quad (\text{eq S6})$$

Table S1 Average ($\pm 1\sigma$) values Abs and MAC of WS-BrC and WI-BrC at the wavelength of 340 nm, 350 nm, 360 nm, 370 nm, and 380 nm in the PM_{2.5} aerosols from the rural site of Guanzhong Basin.

	<u>340 nm</u>		<u>350 nm</u>		<u>360 nm</u>		<u>370 nm</u>		<u>380 nm</u>	
	Summer	Winter	Summer	Winter	Summer	Winter	Summer	Winter	Summer	Winter
<u>Abs_{WS-BrC} (Mm⁻¹)</u>	<u>6.55±1.91</u>	<u>27.5±12.4</u>	<u>5.55±1.61</u>	<u>23.36±10.6</u>	<u>5.27±1.36</u>	<u>20.7±9.02</u>	<u>4.34±1.17</u>	<u>17.8±7.59</u>	<u>3.55±0.99</u>	<u>15.07±6.41</u>
<u>Abs_{WI-BrC} (Mm⁻¹)</u>	<u>4.22±2.67</u>	<u>33.6±20.5</u>	<u>3.61±2.3</u>	<u>28.0±17.1</u>	<u>3.19±2.04</u>	<u>23.9±14.61</u>	<u>2.87±1.81</u>	<u>20.1±12.4</u>	<u>2.63±1.64</u>	<u>17.5±10.8</u>
<u>MAC_{WS-BrC} (m² g⁻¹)</u>	<u>1.29±0.22</u>	<u>1.29±0.34</u>	<u>1.10±0.19</u>	<u>1.09±0.29</u>	<u>1.05±0.18</u>	<u>0.97±0.26</u>	<u>0.87±0.15</u>	<u>0.85±0.23</u>	<u>0.71±0.13</u>	<u>0.71±0.2</u>
<u>MAC_{WI-BrC} (m² g⁻¹)</u>	<u>2.60±1.42</u>	<u>1.46±0.51</u>	<u>2.23±1.24</u>	<u>1.21±0.42</u>	<u>1.97±1.11</u>	<u>1.03±0.35</u>	<u>1.79±1.00</u>	<u>0.87±0.29</u>	<u>1.64±0.92</u>	<u>0.76±0.25</u>

Table S1-S2 Molecular concentrations of the measured parent-PAHs, OPAHs, nitrophenols, and isoprene and α -/ β -pinene derived products in the PM_{2.5} samples in the rural site of Northwest China during summer and winter.

	Summer			Winter		
	Average	Daytime	Nighttime	Average	Daytime	Nighttime
(a) parent-PAHs						
phenanthrene	0.68±0.33	0.64±0.39	0.73±0.26	6.67±3.78	5.64±2.02	7.7±4.73
anthracene	0.05±0.01	0.05±0.01	0.05±0.02	0.38±0.14	0.38±0.14	0.38±0.14
fluoranthene	0.36±0.13	0.36±0.12	0.37±0.14	5.92±3.29	5.68±2.78	6.15±3.71
pyrene	0.34±0.12	0.36±0.14	0.32±0.1	5.84±3.4	5.4±2.6	6.28±4
benz(a)anthracene	0.29±0.13	0.33±0.13	0.26±0.12	5.39±4.18	4.09±2.25	6.69±5.15
chrysene / triphenylene	0.61±0.23	0.63±0.23	0.58±0.22	9.55±6.35	8.32±4.5	10.78±7.57
benzo(b)fluoranthene	1.33±0.87	1.76±1.03	0.9±0.31	13.88±9.11	11.8±6.07	15.96±10.97
benzo(k)fluoranthene	0.38±0.24	0.51±0.28	0.26±0.09	3.51±2.24	3.03±1.52	3.98±2.69
benzo(e)pyrene	1.06±0.65	1.38±0.74	0.74±0.31	8.43±5.56	7.23±3.77	9.63±6.7
benzo(a)pyrene	0.66±0.45	0.94±0.47	0.39±0.17	5.21±3.7	4.23±2.28	6.19±4.5
perylene	0.13±0.09	0.19±0.09	0.07±0.03	1.12±0.85	0.84±0.45	1.39±1.04
indeno[123-cd]pyrene	1.41±1.23	2.24±1.27	0.58±0.2	7.72±5.55	6.65±3.55	8.79±6.83
dibenz(a,h)anthracene	0.25±0.17	0.34±0.18	0.16±0.09	1.77±1.38	1.49±0.84	2.05±1.71
benzo(ghi)perylene	1.25±0.98	1.91±1	0.58±0.23	6.95±4.87	6.06±3.24	7.85±5.95
(b) OPAHs						
anthraquinone	1.84±0.36	1.67±0.29	2.01±0.34	34.33±14.3	32.3±10.16	36.35±17.25
benzathrone	1.89±2.11	3.13±2.39	0.64±0.22	14.9±9.84	13.44±6.89	16.36±11.91
benzo(a)anthracene-7,12-dione	0.61±0.35	0.79±0.38	0.43±0.17	6.05±3.81	5.15±2.49	6.95±4.61
5,12-naphthacenequinone	0.32±0.24	0.48±0.26	0.17±0.06	4.14±3.14	3.09±1.78	5.18±3.79
6H-benzo(cd)pyrene-6-one	9.33±11.44	16.95±12.05	1.72±0.67	38.84±29.42	35.42±19.46	42.26±36.45
(c) Nitrophenols						
4-nitrophenol	0.52±0.16	0.45±0.12	0.59±0.17	15.2±10.17	11.08±4.26	19.32±12.44
3-methyl-4-nitrophenol	BDL*	BDL	BDL	9.69±6.18	6.54±1.77	12.84±7.31
4-nitrocatechol	0.42±0.15	0.42±0.16	0.43±0.14	37.79±38.93	18.67±9.87	56.92±46.92
4-methyl-5-nitrocatechol	BDL	BDL	BDL	9.92±10.76	4.78±2.56	15.05±13.12
(d) Isoprene-derived products						
2-methylglyceric acid	4.15±1.35	3.58±1.04	4.73±1.38	BDL	BDL	BDL
2-methylthreitol	3.55±2.3	2.48±1.65	4.61±2.36	BDL	BDL	BDL
2-methylerythritol	10.84±6.31	8.9±5.65	12.79±6.33	BDL	BDL	BDL
(e) α-/β-Pinene derived products						
pinonic acid	3.92±0.97	3.35±0.68	4.5±0.88	BDL	BDL	BDL
pinic acid	3.85±0.96	3.8±0.54	3.9±1.24	BDL	BDL	BDL
3-methyl-1,2,3-butanetricarboxylic acid	14.27±6.38	18±6.16	10.53±3.94	BDL	BDL	BDL

*BDL: below detection limit.

Table S2-S3 The solar-spectrum-weighted individual $MAC_{PAH,av}$, and the contributions of individual parent-PAH and OPAH to WI-BrC light absorption.

	$MAC_{PAH,av}$ ($m^2 g^{-1}$)	Contribution to WI-BrC light absorption (%)			
		Summer		Winter	
		Daytime	Nighttime	Daytime	Nighttime
(a) parent-PAHs					
phenanthrene	0.0256 ^a	0.004±0.004	0.005±0.003	0.003±0.001	0.003±0.001
anthracene	0.2801 ^a	0.003±0.003	0.004±0.002	0.003±0.001	0.002±0.001
fluoranthene	0.2834 ^a	0.019±0.018	0.026±0.016	0.037±0.014	0.026±0.004
pyrene	0.353 ^a	0.021±0.018	0.028±0.016	0.044±0.016	0.032±0.006
benz(a)anthracene	0.2842 ^a	0.014±0.01	0.018±0.01	0.025±0.01	0.025±0.01
chrysene / triphenylene	0.0883 ^a	0.009±0.007	0.012±0.007	0.016±0.006	0.013±0.003
benzo(b)fluoranthene	0.3475 ^a	0.064±0.045	0.076±0.042	0.092±0.031	0.078±0.018
benzo(k)fluoranthene	0.3475 ^b	0.019±0.014	0.022±0.013	0.024±0.008	0.02±0.004
benzo(e)pyrene	0.7709 ^c	0.109±0.072	0.135±0.073	0.124±0.04	0.104±0.024
benzo(a)pyrene	0.7709 ^a	0.07±0.046	0.074±0.046	0.071±0.027	0.063±0.021
perylene	1.7942 ^a	0.032±0.02	0.032±0.02	0.033±0.014	0.032±0.012
indeno[123-cd]pyrene	1.0711 ^d	0.171±0.095	0.152±0.085	0.156±0.057	0.122±0.045
dibenz(a,h)anthracene	0.2842 ^a	0.027±0.014	0.025±0.013	0.024±0.009	0.019±0.006
benzo(ghi)perylene	0.1821 ^a	0.01±0.006	0.011±0.007	0.009±0.004	0.007±0.003
subtotal		0.57±0.35	0.62±0.34	0.66±0.23	0.55±0.15
(b) OPAHs					
anthraquinone	0.1032 ^a	0.037±0.03	0.051±0.025	0.083±0.023	0.064±0.017
benzathrone	0.4385 ^a	0.082±0.043	0.068±0.04	0.131±0.049	0.097±0.028
benzo(a)anthracene-7,12-dione	0.3069 ^e	0.028±0.02	0.032±0.019	0.036±0.014	0.032±0.006
5,12-naphthacenequinone	0.3069 ^a	0.013±0.007	0.013±0.007	0.021±0.008	0.021±0.008
6H-benzo(cd)pyrene-6-one	0.4385 ^f	0.345±0.243	0.181±0.1	0.336±0.142	0.231±0.101
subtotal		0.51±0.28	0.34±0.19	0.61±0.21	0.44±0.13

^a $MAC_{PAH,av}$ values comes from Samburova et al. (2016) (Samburova et al., 2016); ^b use value from benzo(b)fluoranthene; ^c use value from benzo(a)pyrene; ^d use value from indeno[1,2,3-cd] fluoranthene; ^e use value from 5,12-naphthacenequinone; ^f use value from benzathrone.

Table S3 The contribution (%) of detected individual nitrophenol to light absorption of water-soluble BrC at the wavelength of 365 nm.

	Summer			Winter		
	Average	Daytime	Nighttime	Average	Daytime	Nighttime
4-nitrophenol	0.06±0.02	0.04±0.01	0.07±0.02	0.41±0.16	0.32±0.13	0.49±0.14
3-methyl-4-nitrophenol	BDL ^a	BDL	BDL	0.28±0.13	0.20±0.06	0.36±0.13
4-nitrocatechol	0.06±0.02	0.05±0.01	0.07±0.02	1.30±1.16	0.66±0.25	1.93±1.35
4-methyl-5-nitrocatechol	BDL	BDL	BDL	0.46±0.43	0.23±0.10	0.68±0.50
Total nitrophenols	0.12±0.03	0.10±0.02	0.14±0.02	2.44±1.78	1.41±0.29	3.47±2.03

^a BDL: below detection limit.

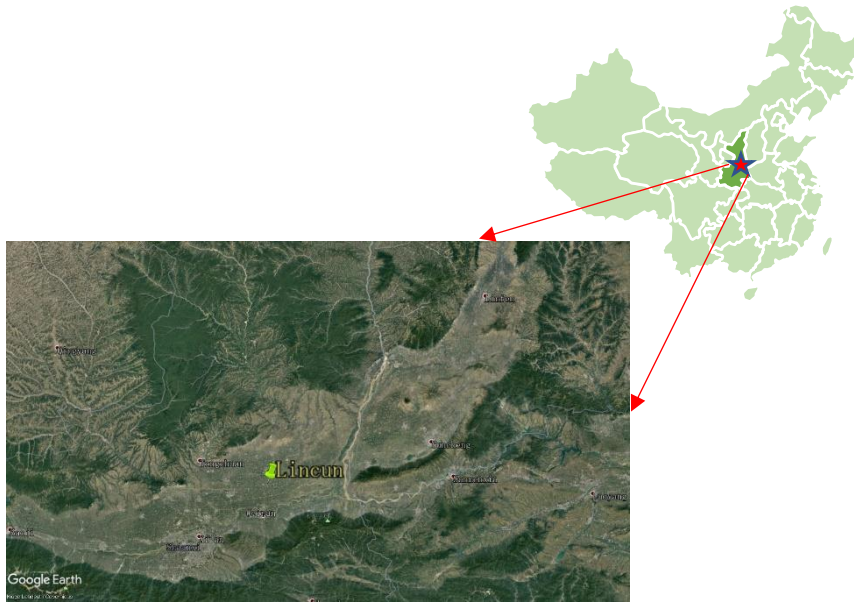


Figure S1 Location of the sampling site (Map data copyright @2019 Google).

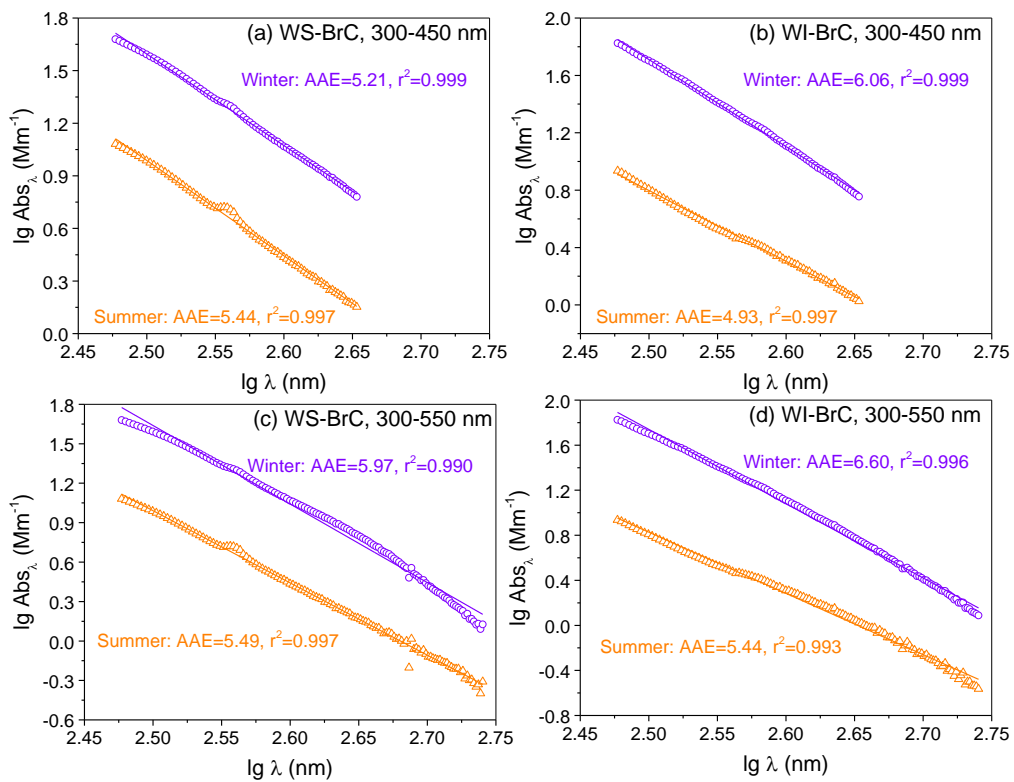


Figure S2 Comparison of Absorption Ångström exponent (AAE) calculation for average absorption spectra in summer and winter in the wavelength of 300-450 nm (a and b) and 300-550 nm (c and d).

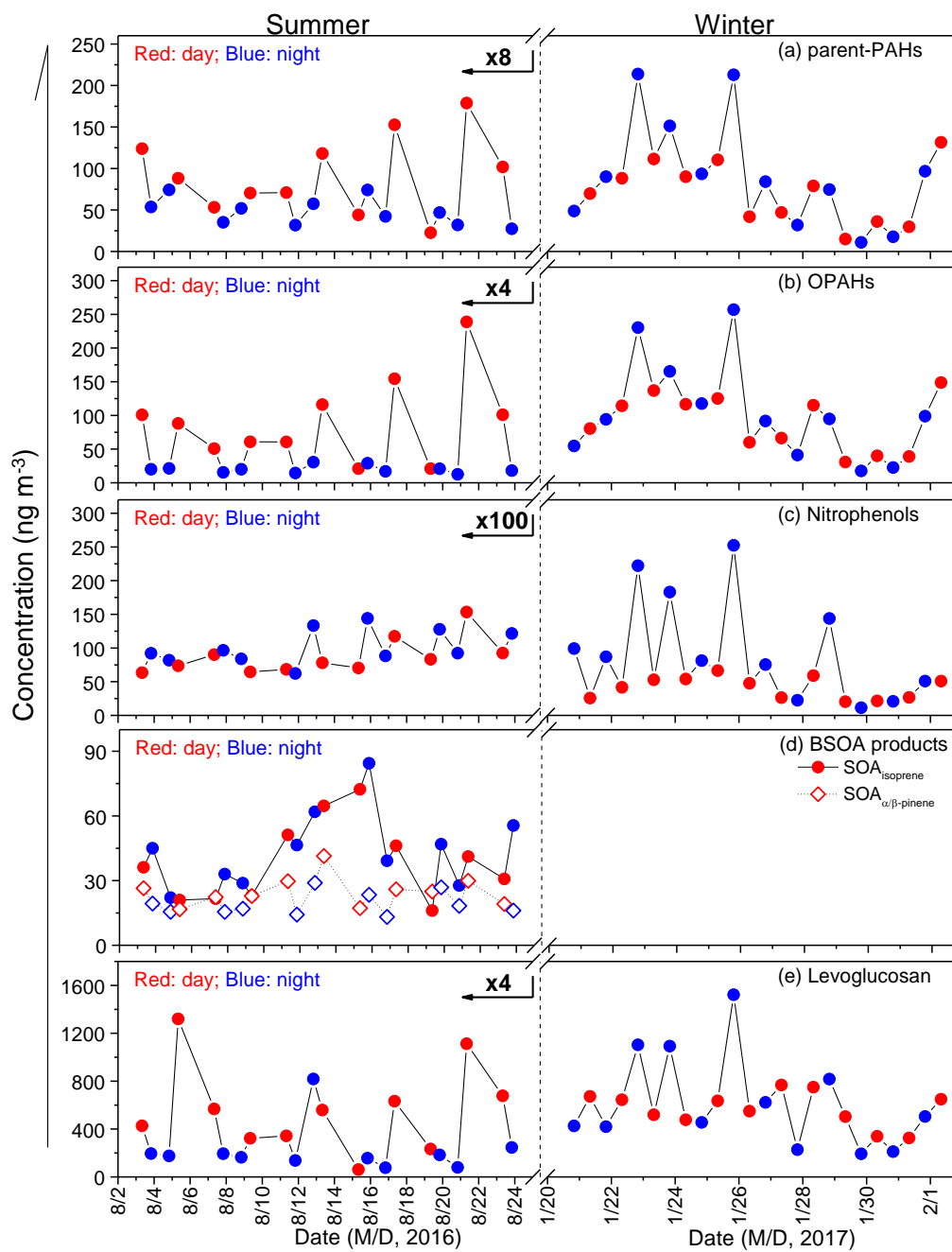


Figure S3 Temporal variation of subtotal concentrations of the measured parent-PAHs (a), OPAHs (b), nitrophenols (c), secondary products derived from isoprene (SOA_{isoprene}) and α - β -pinene ($SOA_{\alpha/\beta\text{-pinene}}$) (d), and levoglucosan (e) in $PM_{2.5}$.

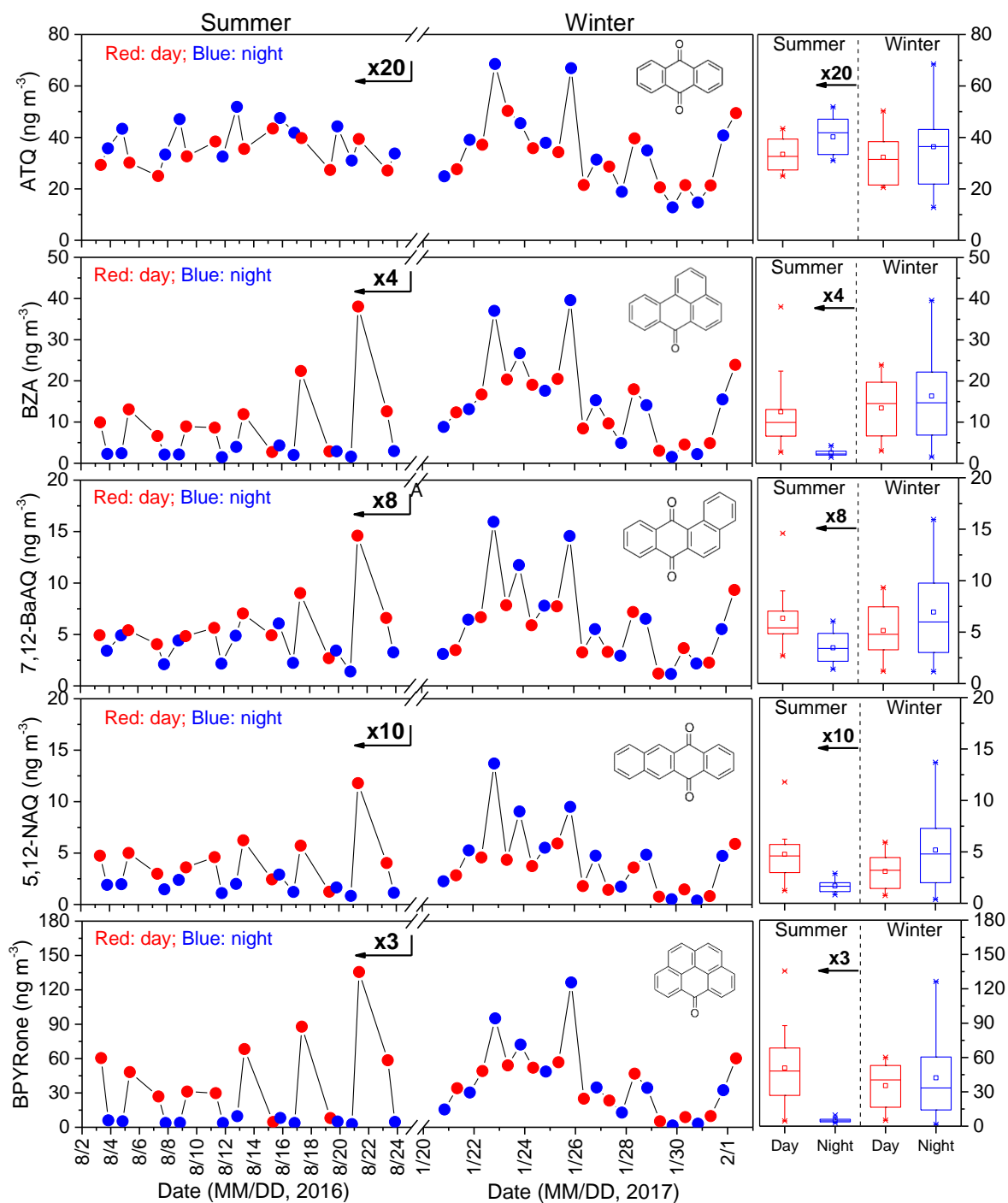


Figure S4 Time series and box charts of the five detected individual oxygenated-PAHs during the sampling period. The number of “ $\times n$ ” in the figures means summer concentrations were lower than winter data by a factor of n .

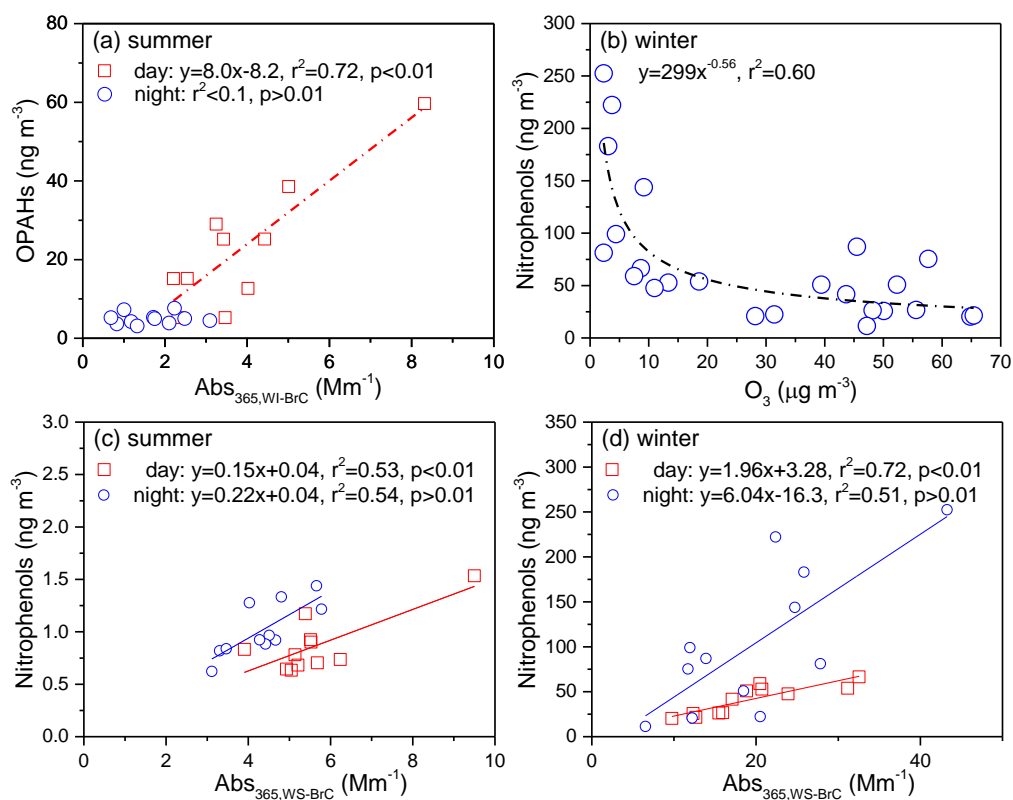


Figure S5 Relationships of OPAHs with Abs_{365,WI-BrC} during daytime and nighttime in summer (a), nitrophenols with O₃ in winter (b), and nitrophenols with Abs_{365,WS-BrC} during daytime and nighttime in summer (c) and winter (d).

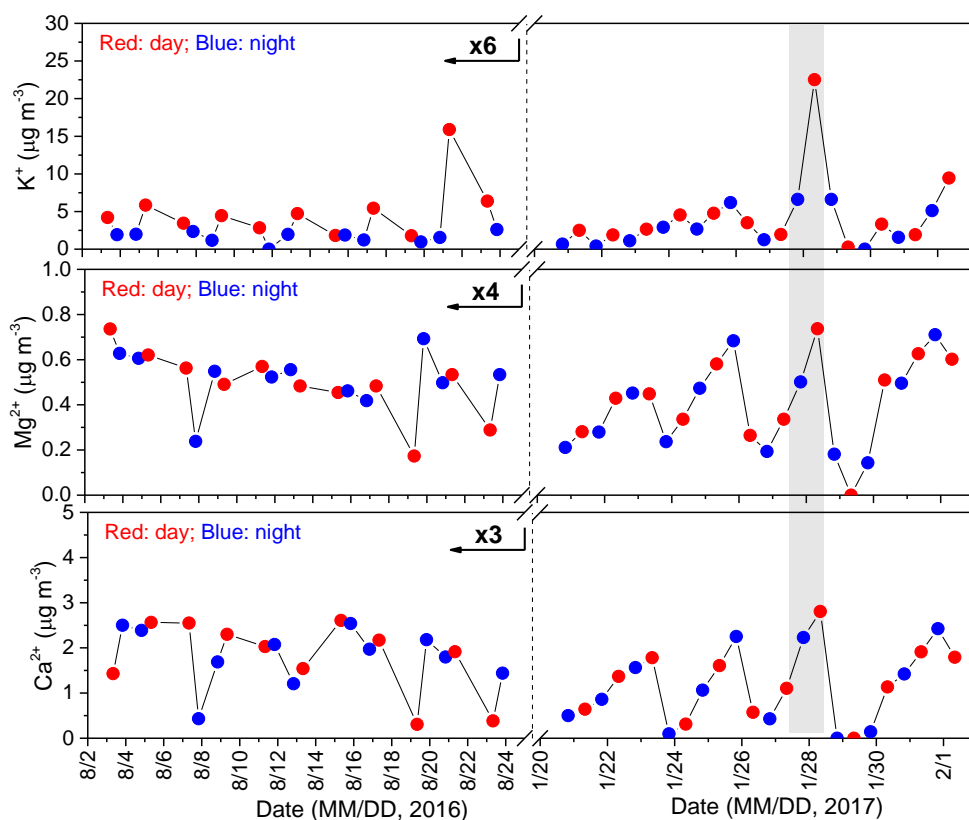


Figure S6 Temporal variation of water-soluble metal ions in PM_{2.5} from the rural area of [location]

Guanzhong Basin. Shadow denotes Chinese New Year eve and Spring festival, during which a large amount of fireworks were set off for celebration.

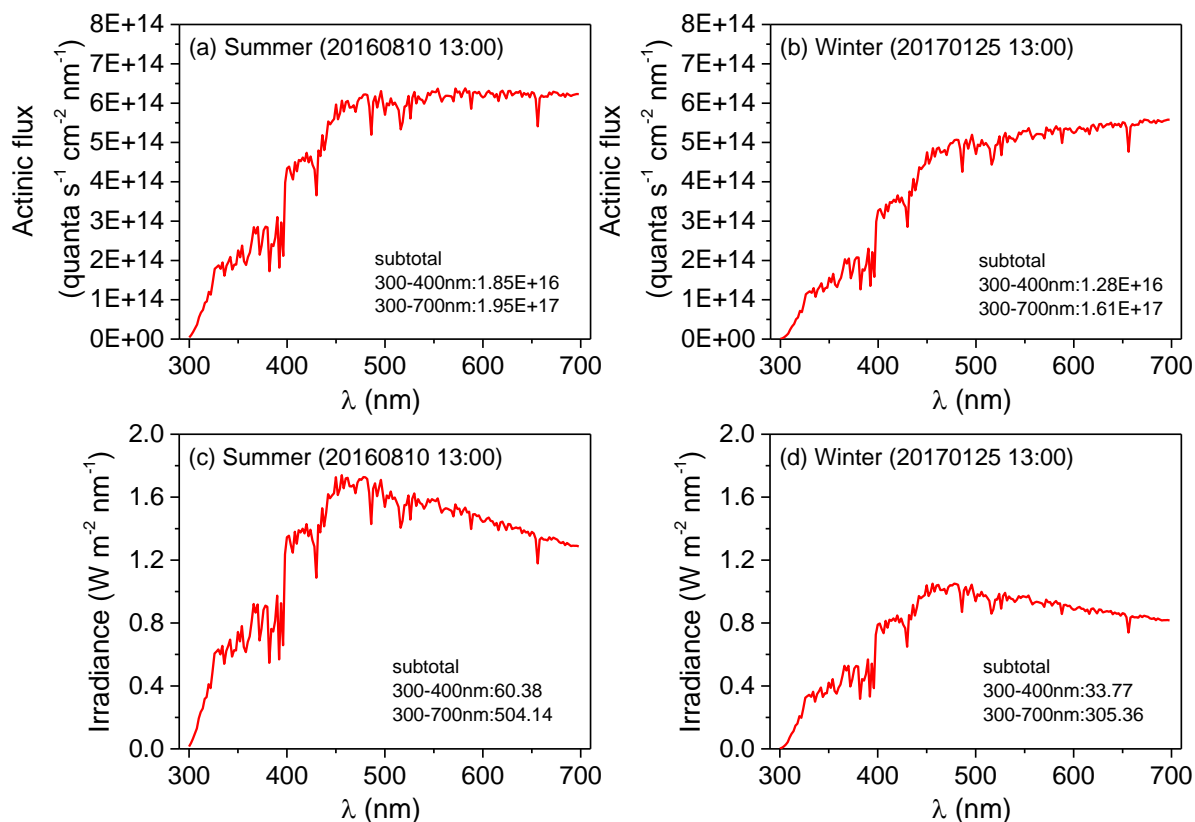


Figure S7 Total down-welling solar spectrum of actinic flux (a and b) and irradiance (c and d) at the sampling site at 20160810 13:00 and 20170125 13:00 (Beijing time) arrived. Data were provided by NCAR TUV Quick Calculator (http://cprm.acom.ucar.edu/Models/TUV/Interactive_TUV/), assuming no cloud effect. Ground elevation is 0.4 km a.s.l. (about 50 m above ground level).

Reference

- Bond, T. C., and Bergstrom, R. W.: Light Absorption by Carbonaceous Particles: An Investigative Review, *Aerosol Science and Technology*, 40, 27-67, 10.1080/02786820500421521, 2006.
- Huang, R.-J., Yang, L., Cao, J., Chen, Y., Chen, Q., Li, Y., Duan, J., Zhu, C., Dai, W., Wang, K., Lin, C., Ni, H., Corbin, J. C., Wu, Y., Zhang, R., Tie, X., Hoffmann, T., O'Dowd, C., and Dusek, U.: Brown Carbon Aerosol in Urban Xi'an, Northwest China: The Composition and Light Absorption Properties, *Environ. Sci. Technol.*, 52, 6825-6833, 10.1021/acs.est.8b02386, 2018.
- Lack, D. A., Bahreini, R., Langridge, J. M., Gilman, J. B., and Middlebrook, A. M.: Brown carbon absorption linked to organic mass tracers in biomass burning particles, *Atmos. Chem. Phys.*, 13, 2415-2422, 10.5194/acp-13-2415-2013, 2013.
- Levinson, R., Akbari, H., and Berdahl, P.: Measuring solar reflectance—Part I: Defining a metric that accurately predicts solar heat gain, *Solar Energy*, 84, 1717-1744, <https://doi.org/10.1016/j.solener.2010.04.018>, 2010.
- Ram, K., and Sarin, M. M.: Absorption Coefficient and Site-Specific Mass Absorption Efficiency of Elemental Carbon in Aerosols over Urban, Rural, and High-Altitude Sites in India, *Environ. Sci. Technol.*, 43, 8233-8239, 10.1021/es9011542, 2009.
- Samburova, V., Connolly, J., Gyawali, M., Yatavelli, R. L. N., Watts, A. C., Chakrabarty, R. K., Zielinska, B., Moosmüller, H., and Khlystov, A.: Polycyclic aromatic hydrocarbons in biomass-burning emissions and their contribution to light absorption and aerosol toxicity, *Science of The Total Environment*, 568, 391-401, <https://doi.org/10.1016/j.scitotenv.2016.06.026>, 2016.
- Sandradewi, J., Prévôt, A. S. H., Weingartner, E., Schmidhauser, R., Gysel, M., and Baltensperger, U.:

A study of wood burning and traffic aerosols in an Alpine valley using a multi-wavelength Aethalometer, *Atmos. Environ.*, 42, 101-112, <https://doi.org/10.1016/j.atmosenv.2007.09.034>, 2008.

Weingartner, E., Saathoff, H., Schnaiter, M., Streit, N., Bitnar, B., and Baltensperger, U.: Absorption of light by soot particles: determination of the absorption coefficient by means of aethalometers, *Journal of Aerosol Science*, 34, 1445-1463, [https://doi.org/10.1016/S0021-8502\(03\)00359-8](https://doi.org/10.1016/S0021-8502(03)00359-8), 2003.